Dynamics of Pulse-Coupled Inhibitory Networks

Master's Thesis

submitted to
Indian Institute of Science Education and Research Pune
in partial fulfillment of the requirements for the
BS-MS Dual Degree Programme

by

Sandeep Chowdhary

Indian Institute of Science Education and Research Pune
Dr. Homi Bhabha Road,
Pashan, Pune 411008, INDIA.

April, 2019

Supervisor: Dr. Collins Assisi

Certificate

This is to certify that this dissertation entitled "Dynamics of Pulse-Coupled Inhibitory Networks" towards the partial fulfilment of the BS-MS dual degree programme at the Indian Institute of Science Education and Research, Pune represents study/work carried out by Sandeep Chowdhary at Indian Institute of Science Education and Research under the supervision of Dr. Collins Assisi, Assistant Professor, Department of Biology , during the academic year 2018-2019.

Dr. Collins Assisi

Committee:

Dr. Collins Assisi

Dr. G. Ambika

This thesis is dedicated to me. And I to it.

Declaration

I hereby declare that the matter embodied in the report entitled "Dynamics of Pulse-Coupled Inhibitory Networks," are the results of the work carried out by me at the Department of Biology, Indian Institute of Science Education and Research, Pune, under the supervision of Dr. Collins Assisi and the same has not been submitted elsewhere for any other degree.

Sandeep Chowdhary

Acknowledgments

I would like to thank my advisor Dr. Collins Assisi for the innumerable meetings and an ever open office door for discussions. This work would not have been possible without his invaluable insights. I would also like to express my gratitude to Dr. Suhita Nadkarni and my lab mates from the Computational Neuroscience Lab for their constructive criticisms and encouragement throughout my time here.

Abstract

In this study, we try to characterize the role inhibition plays in the generation of spatiotemporal patterns that underlie the encoding of odours by the olfactory system and most of the information processing in the cerebral cortex. In the study of network dynamics, the effect of inhibition can be divided into 2 interdependent parts: the connectivity among various neurons (i.e. the structure of the network) and the magnitude of inhibition in the network. We build our work on earlier studies which draw a connection between the dynamics of inhibitory networks and a structural property i.e. the vertex colorings of the inhibitory graph. We find an ideal model for our study in the game of Sudoku. The Sudoku puzzle can be mapped to a graph coloring problem so that the solutions to the empty Sudoku grid are mapped to the 9-colorings of the Sudoku graph. There are $O(10^9)$ solutions of the Sudoku puzzle and thus, there are $O(10^9)$ 9-colorings. We wire a network of pulse-coupled neurons that in principle could generate all the 9-colorings of the Sudoku graph. We show empirically that the asymptotic dynamics of the Sudoku network can be classified in terms of the solutions of the empty Sudoku puzzle or equivalently the 9-colorings of the Sudoku graph. We find that the dynamical system has a measure of closeness between colorings i.e. perturbations to the state representing a Sudoku solution lead you to other *near by* solutions. We propose that these dynamical patterns of excitatory-inhibitory pulse coupled networks which are characterized by the colorings of the graph underlying the inhibitory network are the spatiotemporal patterns involved in odour representation and memory. The huge number of such patterns found in our system point to a very high encoding capacity of neuronal networks. The sense of locality in response to perturbations to the state in our system is similar to the associative nature of memory. Lastly, we focus our attention on the role of the magnitude of inhibition on the dynamics. We vary the coupling strengths systematically to find that our system shows a maximization of encoding capacity for a certain ratio of excitation to inhibition.

Contents

List of Figures

Chapter 1

Introduction

Spatiotemporal patterns of neuronal activity encode all perception, action, and memory. These patterns are generated through an interplay of excitatory and inhibitory interactions among neurons. Central Pattern Generators (CPGs), the neuronal networks underlying rhythmic activities such as swimming, the beating of the heart, etc, depend on an inhibition based mechanism to produce the patterned rhythmic output (Marder and Bucher, 2001). The Cerebral cortex, involved in most of the information processing in the brain as well as the integration of sensory inputs, relies on inhibitory circuits to perform its function (Mann and Paulsen, 2007). Inhibition also plays a key role in Locust Olfactory Networks. Odours are represented in the Antennal Lobe in the spatiotemporal activity of the Projection Neurons (PNs). The odour space is very high dimensional and inputs generally tend to be noisy. Despite this, the locust has the ability to differentiate very similar odours with relative ease. This requires the synchronization of groups of PNs which fire at different peaks of the Local Field Potential (LFP). Inhibition is known to bring about this synchronization of the Projection neurons and the spatiotemporal patterning which characterizes an odour (Laurent, 2002).

For something so ubiquitously present, little is known about how the effect of the structure of inhibitory neuronal networks on the dynamical patterns these networks generate. We employ the idealized model of pulse-coupled neurons given by Mirollo and Strogatz (1990) in our study. It has been shown that "all-to-all" excitatory networks of these pulse-coupled neurons synchronize for almost all initial conditions. They go on to argue that even if the

connectivity is not "all-to-all", all neurons asymptotically synchronize as long as the underlying network is connected. A more interesting case occurs when the coupling is inhibitory. While excitatory systems have a unique state of complete synchrony that all initial conditions evolve to, inhibitory "all-to-all" connected systems display a plethora of asymptotic states called splay phase states (Strogatz and Mirollo, 1993). For a N-oscillator system, these splay phase states are characterized by the N-oscillator's phases distributed uniformly on a unit circle. There is multiplicity associated with these states i.e. if there is one splay state then there are $(N-1)!$ dynamically identical states that can be obtained by permuting the oscillators. This leads to the phenomena of attractor crowding as the number of oscillators, N, increases (Wiesenfeld and Hadley ', 1989).

Most of the work on characterizing the dynamics of these systems has been limited to networks with "all-to-all" connectivity and roles of excitation and inhibition are studied in the absence of each other. Thus, all the existing studies do not capture the richness of neuronal dynamics in the cortex where the connectivity is not limited to "all-to-all" and the neuronal population consists of excitatory as well as inhibitory units.

Earlier studies had drawn a link between a structural property of inhibitory networks (its colorings) and the dynamics it constrains (Assisi et al., 2011; Parihar et al., 2017). This connection provides a useful way of looking at the dynamics of cortical networks but characterizing the dynamics of arbitrary random networks this way is a difficult task. The computational complexity of the graph coloring problem is known to be $NP-hard$. The sheer effort involved in finding all the colorings of an arbitrary inhibitory network and understanding the network dynamics in terms of these colorings leaves the approach intractable. As with many complex physical problems, the key lies in figuring out a toy system that is simple enough to work with, but sufficiently complex that it embodies many of the essential components of the original, seemingly intractable system. We discovered that the simple and popular puzzle, Sudoku, was the perfect toy to tinker with.

Interestingly, the Sudoku puzzle can be mapped to a vertex coloring problem on an 81 vertex graph where each 9-coloring is the solution to some Sudoku puzzle (Herzberg and Murty). We wire an inhibitory network that could, in principle, generate all possible solutions of Sudoku puzzles (nearly $O(10^9)$) and study its dynamics. We hypothesize that the patterns that this Sudoku network generates can be mapped to the colorings of the under-

lying inhibitory graph (Herzberg and Murty).

Chapter 2

Methods

2.1 Pulse Coupled Neurons - Mirollo Strogatz Model:

Mirollo and Strogatz generalized the "integrate and fire" model for Cardiac pacemaker cells given by Peskin (Mirollo and Strogatz, 1990). In the model neurons are described as oscillators. An oscillator's state is given by it's phase $\phi(t)$. The phase grows monotonically in time according to $\dot{\phi} = 1$ until it reaches the threshold $\phi_{threshold} = 1$ (fires), is reset to the resting phase $\phi_{resting} = 0$ and a spike is sent to all neurons postsynaptic to the firing neuron. Then, the cycle repeats (see figure 2.1 (a)).

2.1.1 Spike Processing: Emission and Reception

The synaptic interaction among neurons consist of two consecutive events: first, the presynaptic neuron fires an action potential and then, the action potential is received by the postsynaptic neuron after time τ (the delay time). The assumption made in the model is that the interaction between these neurons is mediated by pulses whose effect on the

(a)

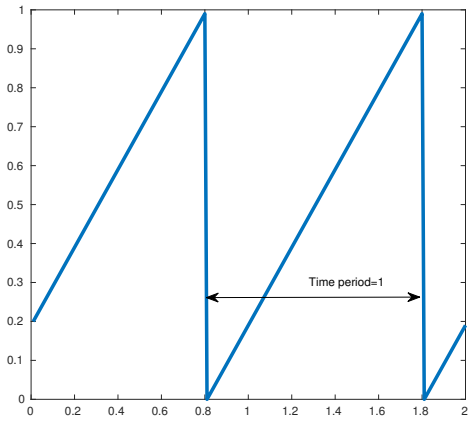

(b)

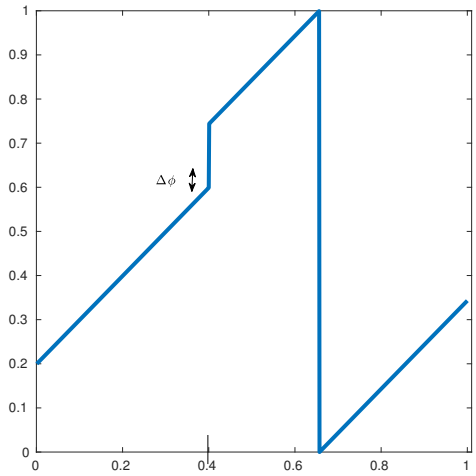

Figure 2.1: Y: phase, X: time. **(a)** Single Neuron Dynamics, **(b)** Effect of an excitatory spike of strength = .01 received at $\phi = .4$. Current $I = 1.01$

postsynaptic oscillators is an infinitely fast phase shift.

This phase shift in the post synaptic neuron(s) is governed by a function $U(\phi)$ which has the following properties:

1. U is concave down i.e $U'' < 0$, (2.1)
2. monotonically increasing($U' > 0$) and
3. normalized such that $U(\phi_{resting} = 0) = 0$ and $U(\phi_{threshold} = 1) = 1$.

Figure 2.2 shows the interaction curve.

2.1.2 State variables of the system with delays

We consider a *small* delay τ in our system and pulses/spikes are received by postsynaptic oscillators/neurons after time τ after the presynaptic neuron spikes. Please note, under this generalization of the model, the state is represented by:

- phases $\phi_i \ \forall \ i = \{1, ..., N\}$ where N is the total number of neurons and
- set of times $t_{i,k} \ \forall \ k = \{1, ..., N_i^{spikes}\}$ where N_i^{spikes} are the total number of spikes travelling in the synapses. Here, $t_{i,k}$ is the time at which the k^{th} spike will reach the postsynaptic neuron i.

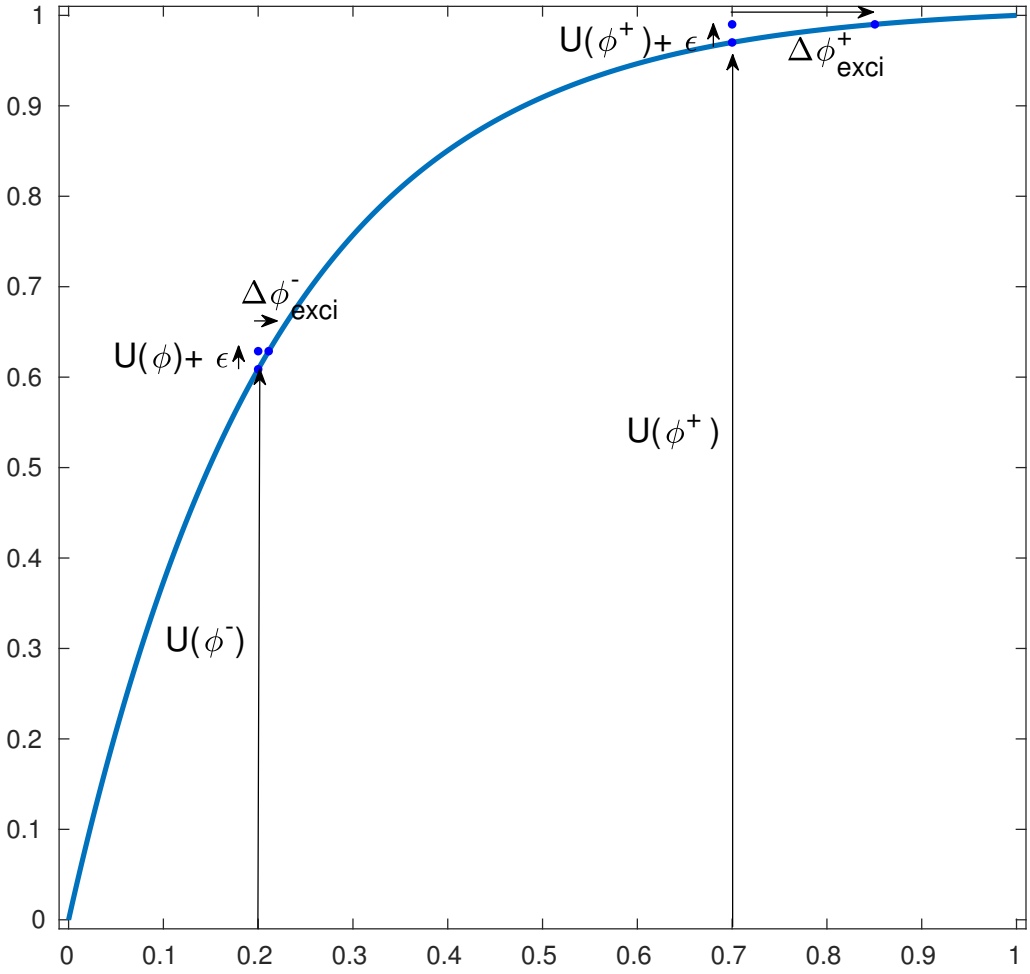

Figure 2.2: Y: $U(\phi)$, X: ϕ. Showing the effect (i.e. $\Delta\phi^-$ and $\Delta\phi^+$) of a pulse of magnitude ϵ at 2 different phases ϕ^-, ϕ^+. Note that $\phi^- < \phi^+ \implies \Delta\phi^- < \Delta\phi^+$.

Say, oscillator i reaches threshold at time t_0 i.e. $\phi_i(t_0^-) = 1$, it is reset to it's resting phase i.e. $\phi_i(t_0) = 0$ and a pulse/spike is sent to all neurons post-synaptic to i i.e. $\forall\ j\epsilon\ Post(i)$ which is received after time τ according to:

$$\phi_j(t = t_0{+}\tau) = \begin{cases} U^{-1}(U(\phi_j(t_0^- + \tau)) + \epsilon_j) & if\ \ U(\phi_j(t_0^- + \tau)) + \epsilon_j < 1 \\ 0 \text{ and a spike is sent to all } Post(j) & if\ \ U(\phi_j(t_0^- + \tau)) + \epsilon_j \geq 1 \end{cases} \quad (2.2)$$

ϵ_j is the pulse size which is determined by the network structure and coupling strengths by $\epsilon_j = \epsilon_j^{exci} + \epsilon_j^{inhi}$ where $\epsilon_j^{exci} = \theta(\sum_k c^{exci} A_{jk}^{exci} \delta_k(t - (t_0 + \tau)))$ and $\epsilon_j^{inhi} = \sum_k c^{inhi} A_{jk}^{inhi} \delta_k(t - (t_0 + \tau))$.
where A_{jk}^{inhi} is the inhibitory adjacency matrix), A_{jk}^{exci} is the excitatory adjacency matrix), c^{exci} the excitatory coupling, c^{inhi} inhibitory coupling and $\theta(x)$ is the excitatory spike response function that controls the effect of excitatory spikes on the post synaptic neurons.

$$\delta_k(t-(t_0+\tau)) = \begin{cases} 1 & if \quad \text{t=t}_0 + \tau \text{ i.e. the } k^{th} \text{ neuron spiked } \tau \text{ time before this event} \\ 0 & otherwise \end{cases}$$

Figure 2.2 shows the variation in the effect of 2 excitatory spikes received at different values of the phase due to the concave down nature of the interaction curve.

We work with $U(\phi) = \frac{I}{\gamma}(1 - e^{T_{IF}\phi})$; where $\gamma = 1$ and the intrinsic period of the oscillator $\quad T_{IF} = \frac{1}{\gamma} log(1 - \frac{\gamma}{I})^{-1} \quad$. But the results are expected to be robust for most functions $U(\phi)$ obeying the conditions labelled (2.1).

2.1.3 Numerical Advantage of the Model: Event Based Update

Apart from being equivalent to several important neuronal models, a notable numerical advantage of pulse coupled systems pointed out by Timme (2002) is that the time evolution of the state need not be done continuously unlike other neuronal models where differential equations need to be integrated over time. Instead, the simulation is done event by event making it considerably more efficient. This *event based update* feature of the model is essential in our study of the asymptotic dynamics of neuronal networks.

Events are of two types:

1. **Threshold Event:** A neuron reaches the threshold phase and emits spikes
2. **Reception Event:** Spikes are received by neuron(s)

2.2 Simulating the system event by event

The time evolution of the system is just determining the next event and changing the phases based on the event. Between consecutive events, the phases of all the neurons grow by the same amount and phase difference among all neurons is a constant frequency is same for all the neurons ($\dot{\phi_i} = 1 \; \forall \; i = \{1, ..., N\}$ where N is the total number of neurons).

To perform the simulation, we calculate time of the next threshold event ($t^{threshold}$) and time of the next reception event ($t^{reception}$).

1. $t^{threshold} = min_i(t_i^{threshold}) \; \forall \; i = \{1, ..., N\}$ where $t_i^{threshold} (= 1 - \phi_i)$ is the time after which the i^{th} neuron will fire.
2. $t^{reception} = min_{i,k}(t_{i,k}^{reception})$ where $t_{i,k}^{reception}$ is the time after which the i^{th} neuron will receive the k^{th} spike (see section 2.1.2, definition of state of the system with delays). As the system has delay between spike emission and reception, a neuron may already have a set of spikes travelling towards it which have not been received.

Now, if $t^{threshold} < t^{reception}$, it's a **threshold event**

- we update the phases ϕ_i to $\phi_i + t^{threshold} \; \forall i$ and the spikes reception times $t_{i,k}^{reception}$ to $t_{i,k}^{reception} - t^{threshold}$
- we set the neurons that reach threshold phase and spike to zero i.e. we set $\phi_j = 0$ if $j : \phi_j + t^{threshold} = 1$,

- we use the adjacency matrix of the network to find all neurons postsynaptic to the spiking neurons i.e. $Post(j)\ \forall j : \phi_j + t^{threshold} = 1$,
- we queue these spikes to be received by the postsynaptic neurons given by $Post(j)$ after the delay time τ.

else $t^{reception} < t^{threshold}$ and it's a **reception event**

- then the spikes are received at time $t + t^{reception}$, we update the phases of the neurons which are receiving spikes according to equations marked (2.2),

  $$\phi_j(t + t^{reception}) = \begin{cases} U^{-1}(U(\phi_j(t + t^{reception})) + \epsilon_j) & if\ \ U(\phi_j(t + t^{reception})) + \epsilon_j < 1 \\ 0 & if\ \ U(\phi_j(t + t^{reception})) + \epsilon_j \geq 1 \end{cases}$$

  ,
  and the spikes reception times $t_{i,k}^{reception}$ to $t_{i,k}^{reception} - t^{reception}$
- neurons k for which $U(\phi_k(t)) + \epsilon_k \geq 1$ fire, get reset and send spikes to their postsynaptic neurons,
- we use the adjacency matrix of the network to find all neurons postsynaptic to the spiking neurons i.e. $Post(k)\ \forall k : U(\phi_k(t)) + \epsilon_k \geq 1$
- we queue these spikes to be received by the postsynaptic neurons given by $Post(k)$ after the delay time τ.

This is one event in the system. The simulation is done by evolving the system through events.

Chapter 3

Results

3.1 Dynamics of Reciprocally Connected Neurons

To elucidate the dynamics of bigger networks we start by understanding the dynamics of small motifs of neurons.

Mutually Excitatory Neurons Synchronize

Mirollo and Strogatz proved that for all initial conditions pair of mutually excitatory pulse coupled neurons synchronize (see figure 3.1). The proof was given under the assumption of infinitely fast transmission of pulses i.e. no delay $\tau = 0$ in the reception of a pulse (Mirollo and Strogatz, 1990).

Proof Outline: The idea behind the proof is that the phase difference decreases over successive *events* (see methods for definition of event). Say, at the n^{th} event one of the oscillator is at phase $\phi_1(n)$ and the other at $\phi_2(n)$. Now, note that the phase difference $\Delta\phi_{1,2}(n)$ $(= min\{|\phi_1(n) - \phi_2(n)|, 1 - |\phi_1(n) - \phi_2(n)|\})$ only changes when there is a spike reception by either of the 2 oscillators as the frequencies of both is the same $(\dot{\phi}_{1,2}(n) = 1)$.

Let's look at change in $\Delta\phi_{1,2}(n)$ over successive events. We look at the case when events $n, n+1, n+2$ are not suprathreshold (an event in which reception of an excitatory spike

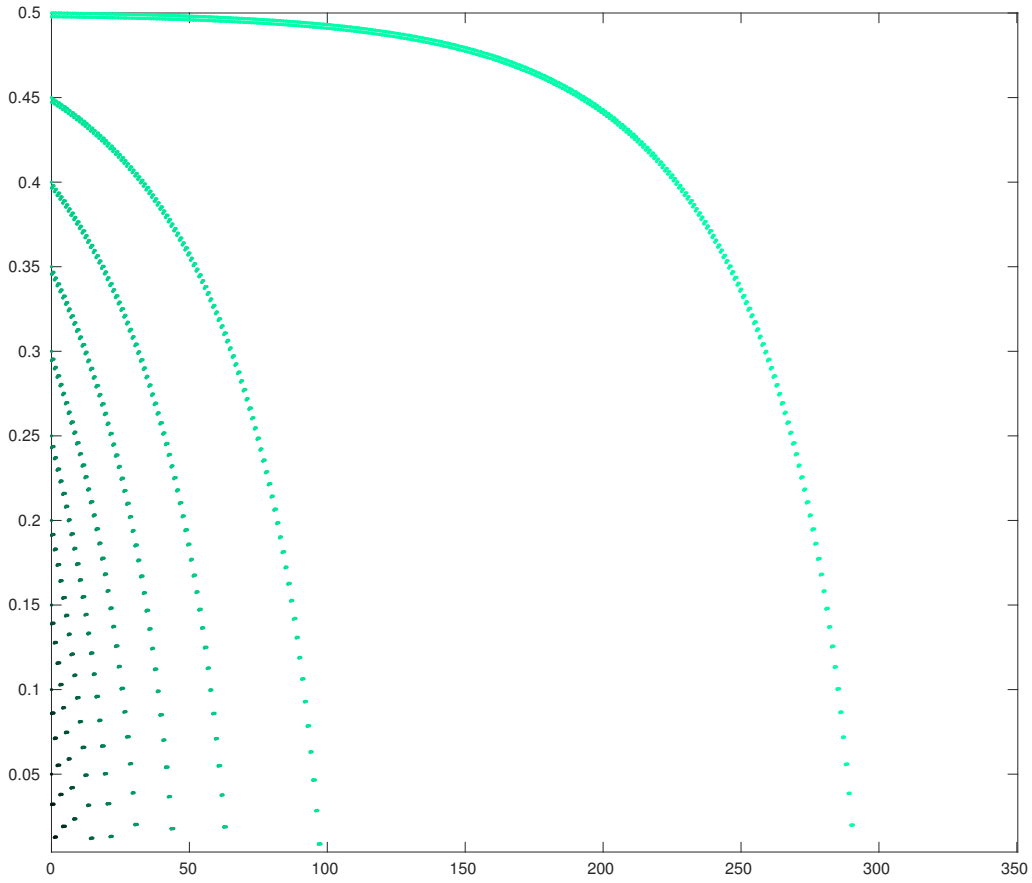

Figure 3.1: Y: phase difference between the pair of the oscillators. X: time (units : T_{free}). Each curve represents an instance of a system 2 reciprocaly exciting neurons. The initial phase difference is varied in the 10 instances from .1 to .5(maximum possible) in steps of0.05. The figure shows that for any initial phase difference, neurons attract and go to the minimum possible phase difference $\Delta\phi_{1,2} \approx 0$ (equality if no delay, $\tau = 0$). Parameters : I=1.01, excitatory coupling $c_{exci} = .001$, delay $\tau = .001$, $\gamma = 1$, frequency $\omega = 1$

causes the postsynaptic neuron to cross the threshold and spike in the same event) because in case of a suprathreshold event, the neurons synchronize immediately and $\Delta\phi_{1,2}(n)$=0. We can assume without the loss of generality that $\phi_1(n) > \phi_2(n) > 0.5$, then (oscillator) 1 fires first and a pulse of magnitude ϵ is received by 2. This event decreases $\Delta\phi_{1,2}(n)$ by

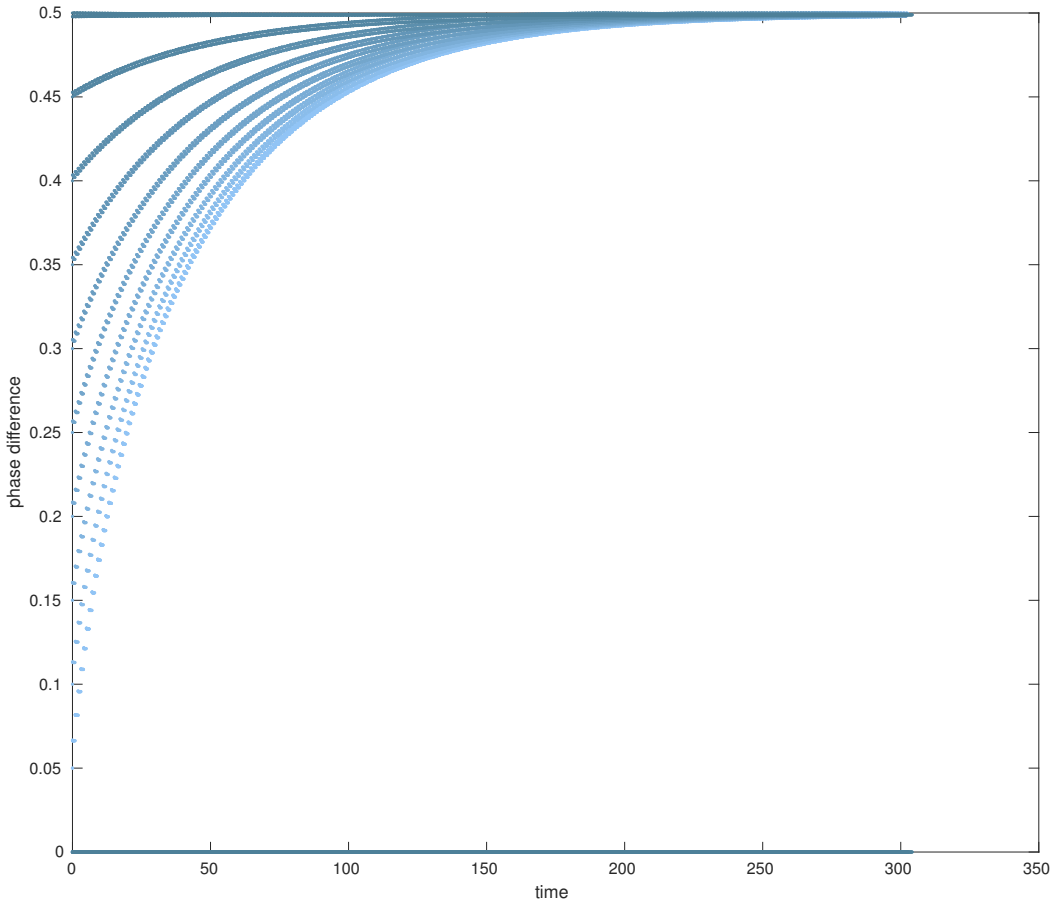

Figure 3.2: Y: phase difference between the pair of the oscillators. X: time (units : T_{free}). Each curve represents an instance of a system 2 reciprocally inhibiting neurons. The initial phase difference is varied in the 10 instances from .1 to .5(maximum possible) in steps of0.05. The figure shows that for any initial phase difference, neurons repel and go to the maximum possible phase difference $\Delta\phi_{1,2} \approx .5$. Parameters : I=1.01, inhibitory coupling $c_{inhi} = .001$, delay $\tau = .001$, $\gamma = 1$, frequency $\omega = 1$.

$\Delta\phi^{+}_{exci}(\phi_2(n))$ (see figure 2.2) i.e.

$$\Delta\phi_{1,2}(n+1) = \Delta\phi_{1,2}(n) - \Delta\phi^{+}_{exci}(\phi_2(n))$$

The next event is neuron 2 firing and neuron 1 receiving a pulse of magnitude ϵ which increases $\Delta\phi_{1,2}$ by $\Delta\phi^{-}_{exci}(\phi_1(n+1))$ (figure 2.2) i.e.

$$\Delta\phi_{1,2}(n+2) = \Delta\phi_{1,2}(n+1) + \Delta\phi^{-}_{exci}(\phi_1(n+1))$$

So,

$$\Delta\phi_{1,2}(n+2) = \Delta\phi_{1,2}(n) + [\Delta\phi^{-}_{exci}(\phi_1(n+1)) - \Delta\phi^{+}_{exci}(\phi_2(n))]$$

and $\phi_1(n+1) > \phi_2(n)$ as neuron 2 spiked in event $n+1$.

Due to concave down nature of interaction function U, we have $\phi^- < \phi^+ \implies \Delta\phi^- > \Delta\phi^+$ (see figure 2.2). Thus,

$$\Delta\phi^{-}_{exci}(\phi_1(n+1)) < \Delta\phi^{+}_{exci}(\phi_2(n))$$

$$\implies \Delta\phi_{1,2}(n+2) < \Delta\phi_{1,2}(n)$$

We see that $\Delta\phi_{1,2}$ decreases over consecutive events until it goes to 0 in a suprathrehold event. For the proof of synchronization of "all-to-all" excitatory networks, refer to Mirollo and Strogatz (1990). Their simulations show that even if the network is not "all-to-all", as long it's connected, complete synchronization is the asymptotic state.

The assumption of no transmission delay is quite a strong and not very realistic when considering neuronal networks. So, we added a *small* transmission delay to our system. Our simulations show that excitatory neurons synchronize and inhibitory neurons go to anti phase states even in the presence of *small* delays (see figure 3.1 and 3.2, $\tau = .00001$).

Mutually Inhibitory Neurons Do Not Synchronize

Mutual inhibition gives rise to "out of phase" dynamics. Inhibitory neurons don't synchronize, they go to anti phase states or they 'repel' in phase space . The existence of the asymptotic splay phase states has not been proved for pulse coupled model given by Mirollo and Strogatz (1990) but an argument can be made following the same line as the proof for synchronization of excitatory oscillators given in the previous section. i.e. the phase difference $\Delta\phi_{1,2}$ increases on consecutive events (see fig 3.2).

This dynamical behaviour of antagonistic agents is not limited to the Mirollo-Strogatz model.

Assisi et al. (2011) use single compartment Hodgkin-Huxley neurons and show for complete k-partite networks and other variants that the dynamics of inhibitory networks can be characterized by the colorings. But the network variants considered in the study posses very few colorings. Parihar et al. (2017) employ VO_2 based coupled relaxation oscillators to solve the minimum coloring problem using inhibitory interactions. Here, the focus is on the possibility of using distributed dynamical system to solve computationally hard problems such as minimal graph coloring problem. The study does not describe the effect of multiple allowed colorings on network dynamics.

Inspired by these studies, we looked for a network with large number of allowed colorings. We found an ideal candidate in the game of Sudoku which could be mapped to a graph coloring problem. The number of Sudoku solutions of the empty grid and equivalently 9-colorings of the graph coloring problem is $\approx 10^9$, a huge number. In the next section, we describe the game of Sudoku and map it to a graph coloring problem.

3.2 Game of Sudoku

The widely popular game of Sudoku is played on a 9 x 9 grid (Figure 3.3). The 9 x 9 grid consists of nine 3 x 3 sub-grids. A Sudoku puzzle consists of a 9 x 9 grid partially filled with numbers 1 to 9. The aim is to fill numbers (from 1 to 9) at the empty locations in the grid until none remain, while respecting the following rules: each row, column and 3 x 3 sub grid must have numbers 1 to 9. The rules ensure that numbers are not repeated in any row, column or sub grid (figure 3.5 highlights the row, column and sub-grid in white).

3.2.1 Sudoku as a Graph Coloring Problem

Constructing the Sudoku graph

Let's construct a graph as follows:
1. **Vertex Set**: Label all the 81 squares in a Sudoku puzzle with numbers 1 to 81 in the

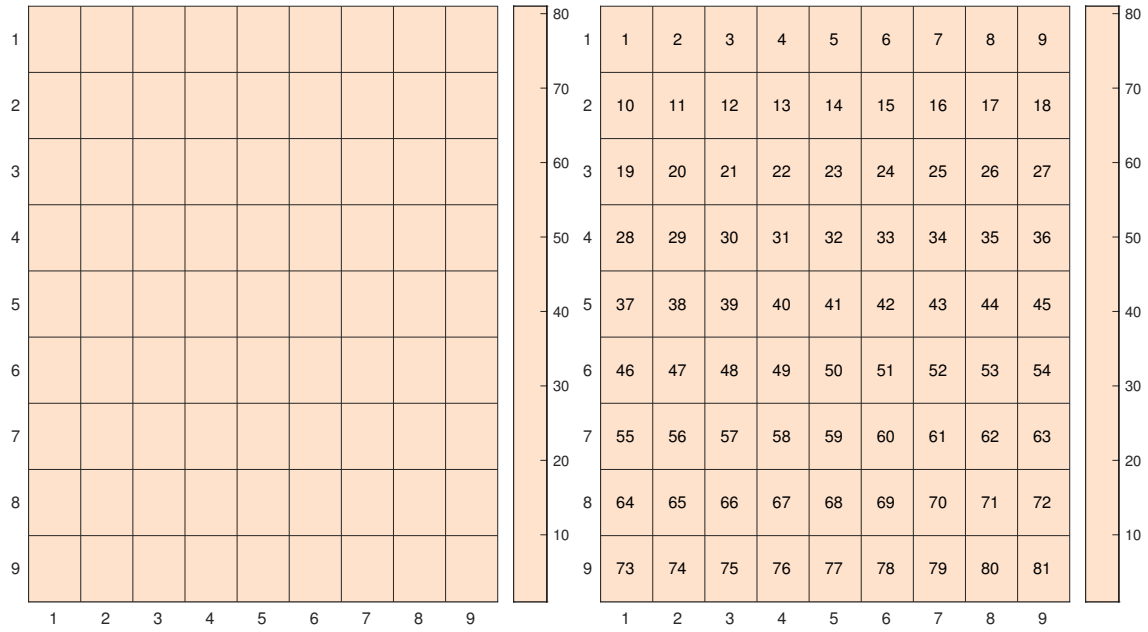

Figure 3.3: Left: Empty Sudoku puzzle (no clues), Right: Labelling Sudoku grids 1 to 81.

way shown in fig 3.3. Then, define the vertex set by mapping each of the 81 squares to a vertex. So, the vertex set of graph G_{Sudoku} is given by V(G)=$\{v_1, v_2, ...v_{81}\}$.

2. **Adjacency Matrix:** Two vertices v_i and v_j are connected i.e. $A_{i,j}(G_{Sudoku})$=1, if they belong to the same column, same row or same 3x3 sub-grid of the empty Sudoku grid where A is the adjacency/connectivity matrix (see Figure 3.4).

We call this the Sudoku graph.

Mapping Sudoku solutions to colorings of the Sudoku graph

Graph Colorings Let G=G(V, E) be a graph on the set of vertices V and set of edges E. Then, a k-coloring of G is defined as *a grouping of vertices into k partitions $P_1, P_2, P_3, ..., P_k$ such that inside any partition P_i, there are no edges connecting any two vertices.*

The claim is that the 9-colorings of this graph has a one to one mapping to the solutions of the empty Sudoku puzzle which have been found to be $O(10^9)$ (Herzberg and Murty). This follows from the way we have constructed the Sudoku graph.

(a)

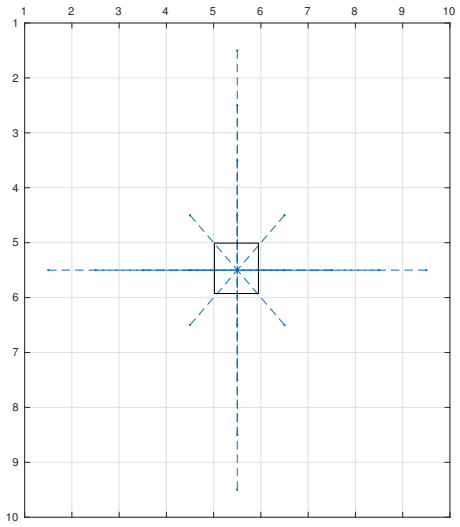

(b)

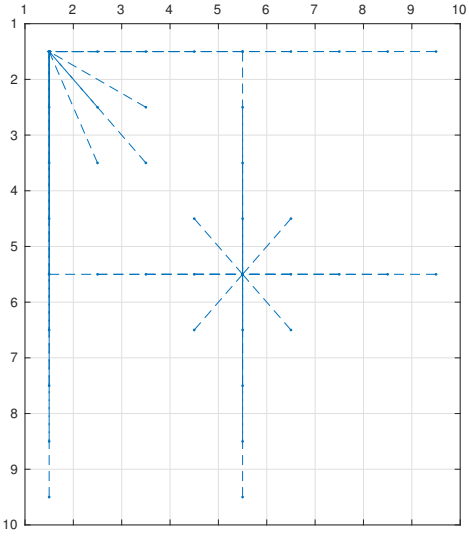

(c)

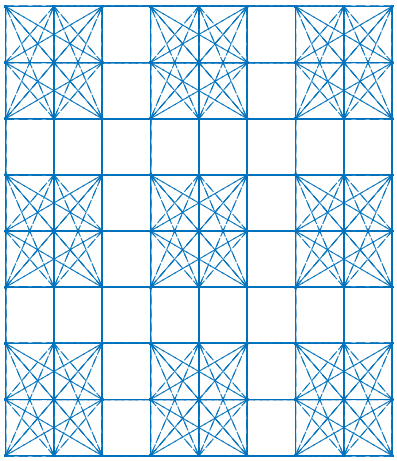

Figure 3.4: Constructing the Sudoku graph. **(a)** All edges for vertex 41 (label as in fig 2.2), **(b)** adding edges for vertex 1, **(c)** adding the edge for all 81 vertices, we arrive at the empty Sudoku graph.

Any Sudoku solution S can be expressed by $s_i \epsilon \{1, 2, ..., 9\}$ for $i \epsilon \{1, 2, 3, ..., 81\}$ where i refers to the label of a box inside the Sudoku puzzle (as in Figure 3.3: Right Panel) and s_i is the number inside the box.

Associated coloring C is obtained by putting all the vertices with same s_i in the same partition. This way one arrives at 9 partitions. Now note that any vertex has connections only with vertices in the same row, column or sub-grid as in figure 3.4 and the condition for S to be a solution is that no numbers can occur twice in the same row, column or sub-grid. Thus, there can be no edges between vertices labeled by the same s_i and C must be a coloring of the Sudoku graph/network.

3.2.2 Structural Properties of Sudoku Graph G_{Sudoku}

1. Each vertex in this network/graph has degree 20. This is obvious from the way the network was constructed. We connected each vertex to all the vertices in the same row, same column, and same 3x3 sub-grid. So, total neighbors for any vertex is 20 (see the boxes in white rectangles in figure 3.12).
2. The graph is symmetric.
3. The chromatic number(minimum number of colors required to color the graph) is 9.
4. Every solution of the Sudoku puzzle is a 9-coloring of the empty Sudoku network.

3.3 Creating the Dynamical System

Now we construct the Sudoku network which we will use to demonstrate the characterization of asymptotic dynamics in terms of the network's colorings.

We map the Sudoku graph G_{Sudoku} to a dynamical system by mapping each vertex to pulse coupled neuron/oscillator and all the edges are mapped to inhibitory connections/synapses. So, adjacency matrix of the inhibitory graph A^{inhi}=$A(G_{Sudoku})$. In addition, we have the excitatory network $A^{exci} = \bar{A}^{inhi}$ where $\bar{A}$ is the adjacency matrix of the complement graph obtained from A by putting all ones to zeros and zeros to ones. The excitatory graph is just the complement of the inhibitory graph. Note that there are no self connections i.e. $A^{inhi}_{ii} = A^{exci}_{ii} = 0 \ \forall i$.

For all Sudoku related results, we take the excitatory spike response function $\theta(x)$ (see

methods for definition) to be a step function i.e. $\theta(x) = \begin{cases} 0 \text{ if } x = 0 \\ 1 \text{ if } x > 0 \end{cases}$

This is equivalent to saying that multiple excitatory spikes (> 1) received at a single event are treated as one spike. This is an important caveat of our system.

This is done to obtain a dynamical system with perfect colorings. This allows us to map dynamics to solutions of Sudoku and analyze the phase space structure in terms of Sudoku solutions.

In general, the response to multiple spikes is not equal to the response to one spike but nor is it additive. Mirollo and Strogatz state: "it seems improbable that 10 fireflies flashing simultaneously would have 10 times the effect that one would have." (Mirollo and Strogatz (1990), section 3.4).

The model was originally based on the flashing of fireflies but even in the context of neurons, it is presumable that the response is sub-linear. We expect that the results will be valid for a sufficiently sub-linear excitatory spike response function $\theta(x)$.

3.4 Sudoku Dynamics

We extrapolate on our understanding of the dynamics of a pair of inhibitory neurons and a pair of excitatory neurons (see section 3.1) to gain an intuition for the dynamics of the Sudoku network.

Role of Inhibitory Network: Any 2 neurons connected in this network will 'repel' one another in state space (see fig 3.1). Thus, states in which none of the neurons that inhibit each are far apart will be stable.

Role of complementary Excitatory Network: The neurons that do not inhibit each other excite each other(by the definition of A^{exci} see section 3.3) and evolve towards synchronization.

Through this interplay of excitation and inhibition, the system effectively evolves towards states where neurons that are not connected in the inhibitory network (or equivalently in the Sudoku graph G_{Sudoku}), fire close (synchronously even) to each other in phase space. For a range of coupling strengths such that the ratio of excitatory and inhibitory coupling c^{exci}/c^{inhi} is $O(1)$, the neurons form 9− groups/partitions firing sequentially, separated from each other in phase space such that all the inhibitory connections are across and none inside the groups. Then, the system's state can be mapped to a $9-coloring$ of G_{Sudoku} using algorithm in section 3.4.1. As c^{exci}/c^{inhi} increases, the clustering of neurons increases and number of partitions i.e. k decreases (see section 3.7 for detailed explanation).

Of course, the argument is heuristic, the idea of emergence i.e. "whole may be greater than the sum of parts" may play a role and the local stability of each inhibitory oscillator pair may not imply the stability of the network of oscillators. But simulations agree with the argument.

3.4.1 Algorithm for Coloring identification

To identify the 9-coloring associated with the state of the dynamical system, we apply the following algorithm:

- We pick the oscillator labelled 1 to 9 (see figure 3.3) to be in 9 separate partitions. These vertices are connected all to all (see figure 3.4) and by the definition of graph coloring, can never be together in any coloring of the network.

- Next, we calculate the phase difference of all the oscillators from these 9 vertices $\Delta\phi_{i,j}(e) = min\{|\phi_i(e) - \phi_j(e)|, 1 - |\phi_i(e) - \phi_j(e)|\}$ where $i\epsilon\ 1, 2, ..., 9$, $j\epsilon\ \{1, 2, 3, ..., 81\}$ and e is the event. We average the phase difference over a few events $\sim O(100)$.

- For each oscillator i from 1 to 9, we put 8 oscillators with the *least* average phase difference $\Delta\phi_{i,j}$ from oscillator i into the partition P_i containing oscillator i. Now, every oscillator from 1 to 81 belongs to a partition.

- If there is no partition P_i, $i\epsilon\ 1, 2, ..., 9$ such that any vertices $v_\alpha, v_\beta \epsilon P_i$ are connected, then the dynamical system has arrived at a coloring.

3.4.2 Colorings and Associated Sudoku solutions

We study the asymptotic dynamics by choosing random initial phases for the 81 oscillators picked from a uniform distribution over 0 to 1 (see figure 3.5 and 3.6) and evolving the dynamical system for a large number of *events* (see methods for definition). The oscillators form clusters and keep changing their neighbors until they find themselves in an allowed coloring of the system In figure 3.15, we plot the number of times system arrives at a coloring for 500 random initial phases of the 81 oscillators generated using MATLAB rand(81,1) function with seeds 1 to 500. One can see that the system arrives at colorings for a large fraction of the total instantiations of the system.

Asymptotic states *close* to proper colorings

We note that there are initial states for which the system gets *stuck* in imperfect colorings — which are *close* to the allowed 9 colorings. Close in the sense that if we cluster them using the algorithm given in section 3.4.1 then a few partitions have inhibitory connections/edges among its constituent neurons/vertices, and hence the state is not a perfect colouring but close to one. In Figure 3.14, it's evident that the number of coloring increases on application of small perturbations. That is, some of the imperfect colorings that the system gets stuck in also arrive at proper colorings. We elucidate this role of noise in the system in section 4.2.

Dynamics at a Solution/Coloring

At a coloring the 81 neurons are separated into 9 partitions (see figure 3.5 (c), 3.6 (c). These 9 partitions have 9 neurons each all of which excite each other (by the definition of a coloring there are no inhibitions within a partition).
We analyze the dynamics of the coloring shown in figure 3.5 (c) to pave way for the argument

(a)

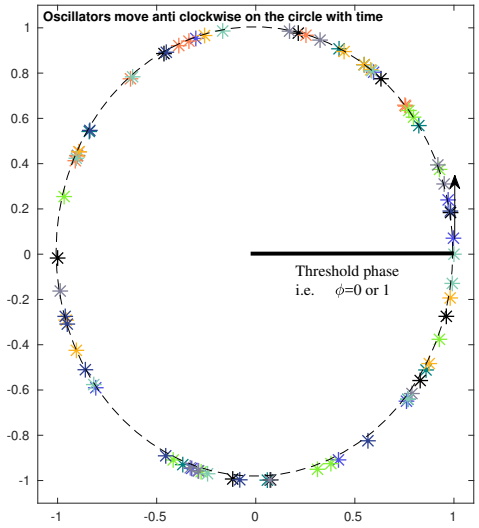

(b)

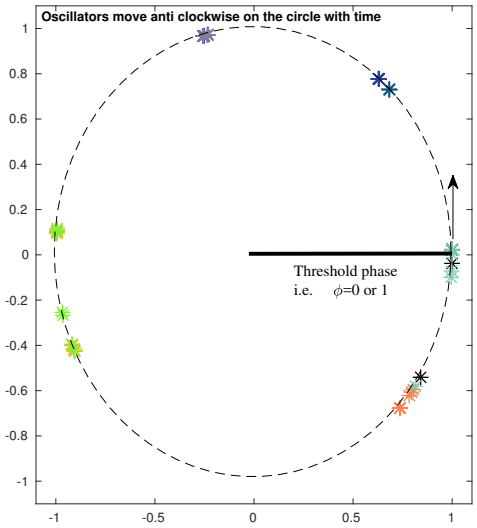

Figure 3.5: Dynamics of the 81 oscillators can be understood as the oscillators rotating anticlockwise on a circle with uniform velocity unless a spike is received. The colors represent the final identities of the neurons. For example, all the orange neurons cluster together in the asymptotic state. See fig 3.8 (c) (next page). **(a)** The initial state: one can see that there is no clustering of neurons. **(b)** After $1.2\text{x}10^4$ events, we see that some neurons have formed clusters. Some neurons of orange and the green partitions are already synchronized and separated from the rest of the neurons. The system goes through a transient in which neurons synchronize and desynchronize, eventually ending up into a coloring state. **(c)** Dynamics after $2\text{x}10^4$ *events* or $461T_{free}$ (on next page): the system arrives at a valid coloring of G_{Sudoku}. The 9 partitions keep going around the circle sequentially.

Fig 3.5(c)

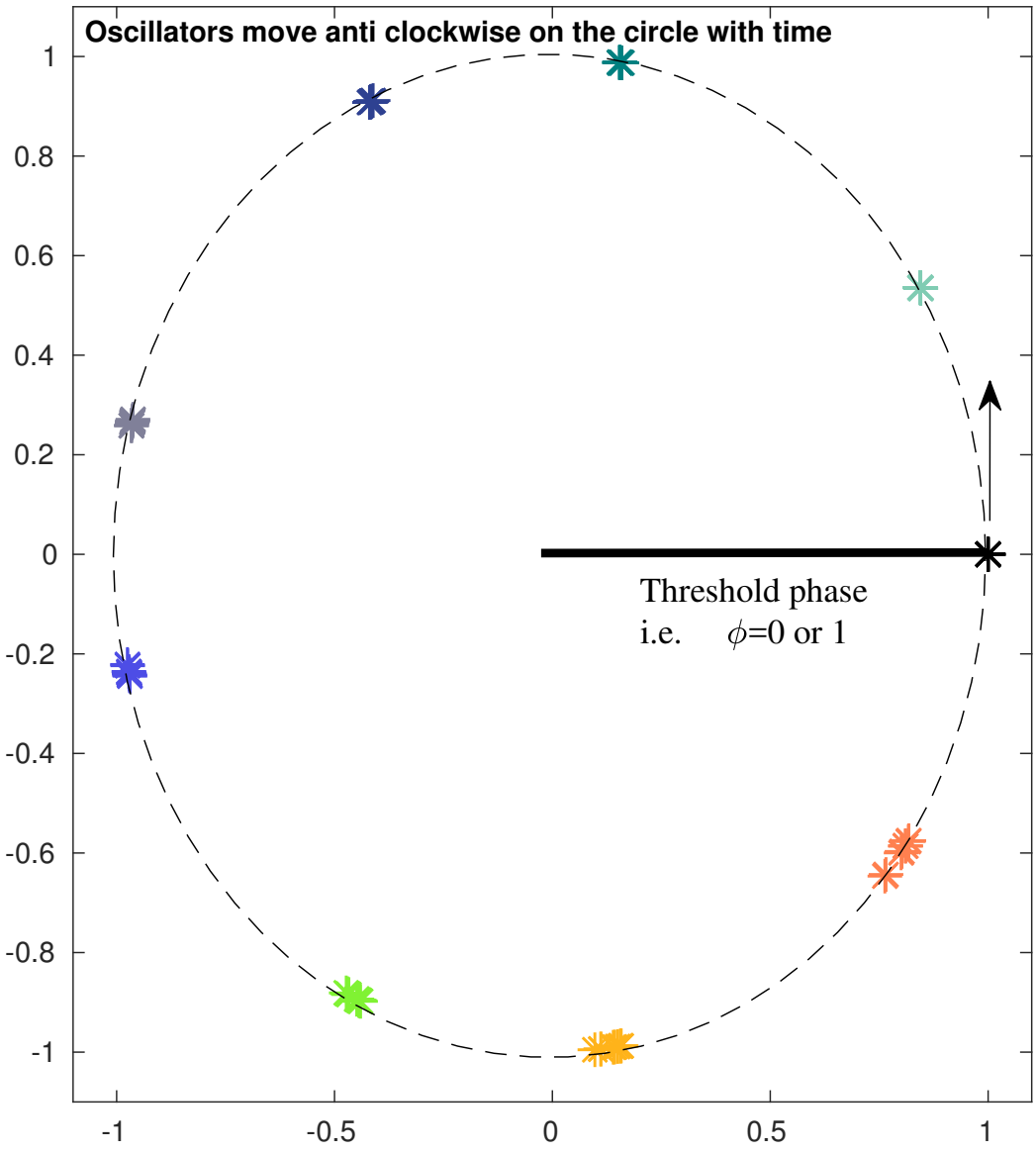
Oscillators move anti clockwise on the circle with time
Threshold phase
i.e. ϕ=0 or 1
1
0.8
0.6
0.4
0.2
0
-0.2
-0.4
-0.6
-0.8
-1
-1
-0.5
0
0.5
1

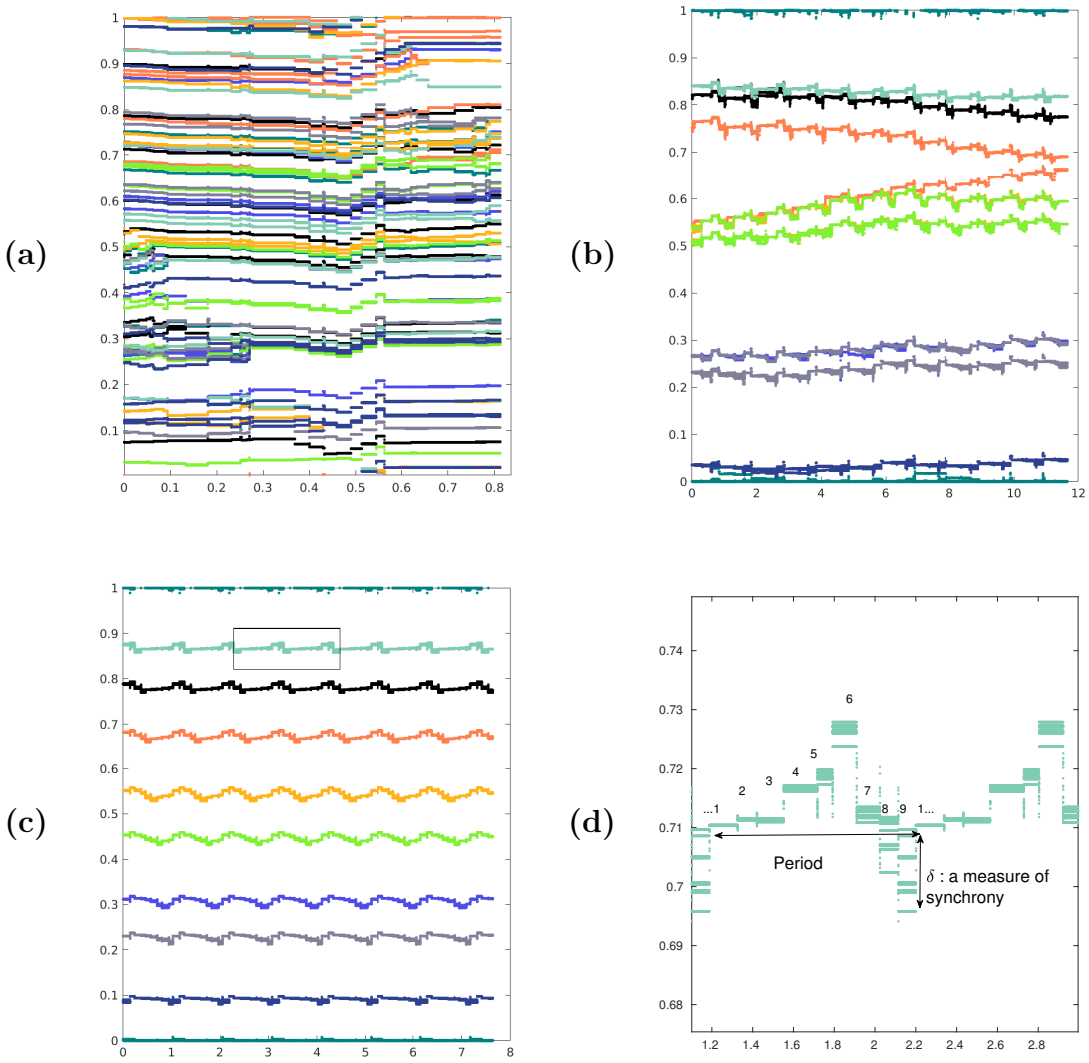

Figure 3.6: Y: the phase difference $\Delta\phi_{a,reference}$, $a\epsilon 1, ..., 81$ of 81 oscillators from reference oscillator, chosen to be oscillator 1 (see figure 3.3). X: time (unit: T_{free}). **(a)** The initial state: no obvious clustering of oscillator is observed, **(b)** After 10^4 events, some clusters form but they do not represent a coloring. The system hasn't settled. **(c)** Dynamics after $2\text{x}10^4$ *events* or $416T_{free}$. The system has arrived at a valid Coloring C and maintains itself there. **(d)** shows how the partition splits apart (desynchronizes) when the neurons in the other 8 partitions fire and then resynchronizes as the it fires and excites all the neurons to thresholding.

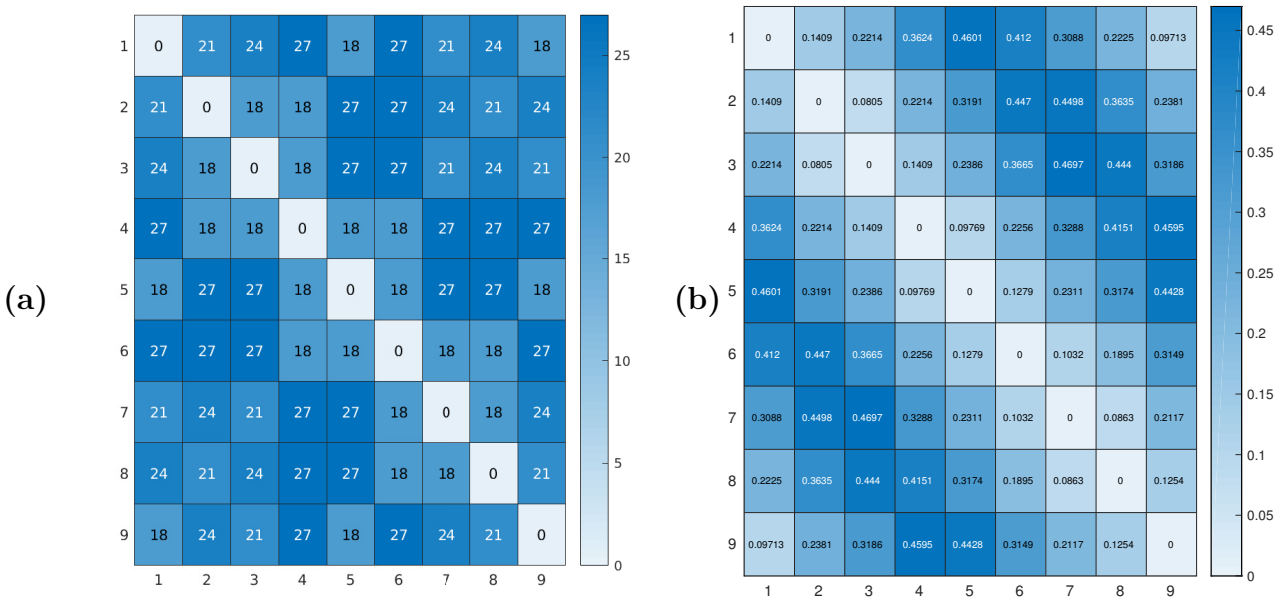

Figure 3.7: Matrix of inhibitions $J(C)$ (see section 3.7.2) and $D(C)$ for the coloring obtained in Fig 3.6 and 3.7: **(a)** $J(C)$: $J_{P,P'}(C)$ is the number of inhibitory connections between partition P and P' when the system is in the coloring C. The matrices have been ordered according the firing order of the partitions. It can be seen that the partitions that fire next to each other inhibit each other the least i.e. $J_{P,P\pm1} = 18$ **(b)**$D(C)$: the distance matrix where $D_{P,P'}$ is the average phase difference between the oscillators of partition P and P'. As the partitions are arranged according to the firing order of partitions for Coloring obtained in Fig 3.6 and 3.7, thus $D_{P,P\pm1}$ are the minimum distances for any partition $P\epsilon\{1, 2, ..., 9\}$.

on the stability of colorings based on the J matrix (see Section 3.7.2.2). We do this event by event:

- **Event 1:** Let the first event be a neuron of the sky blue partition (or partition 9) reaching threshold (as shown in figure 3.6 (c),(d)).

- **Event 2:** The remaining 8 neurons receive excitatory spikes after some delay $\tau = 10^{-5}$, their phases increases by $\Delta\phi^{+}_{i,skyblue}$ (see figure 2.2) and they spike on the reception of these spikes from the first sky blue neuron and synchronize.

- **Event 3:**

  - The first neuron now receives spikes from the 8 neurons that reached threshold τ time before and it's phase increases by $\Delta\phi^{-}_{1,skyblue}$ which is small as $\phi^{-}_{1,skyblue} = \tau = 10^{-5}$ (see figure 2.2). Thus, the neurons of the partition come close in phase space as the partition passes through the threshold.

  - The neurons in any other partition $P' \neq 9, skyblue$ receive inhibitory and excitatory spikes. The number of inhibitory spikes received by any neuron of partition $P' \neq skyblue$ is either 2 or 3 as discussed in section 3.7.2 (5)) and the number of excitatory spikes received by any neuron in P' is either 6 or 7 (as excitatory network is the complement of the inhibitor graph) but they are treated as 1 spike (see definition of *excitatory spike response function* $\theta(x)$ in section 3.3). The response to the inhibitory spikes is higher than that of the excitatory spikes as $c^{inhi} > c^{exci}$. Thus, any neuron in any partition $P' \neq 9, skyblue$ experiences a decrease in it's phase and is effectively pushed away from partition $P = 9, skyblue$. Thus, inter-partition distance increases.

The phase jumps caused by the spikes are progressively lower for partitions with phase to close to 0 and maximum for the ones that are closest to phase of 1. This is due to the concave down nature of the interaction function U.

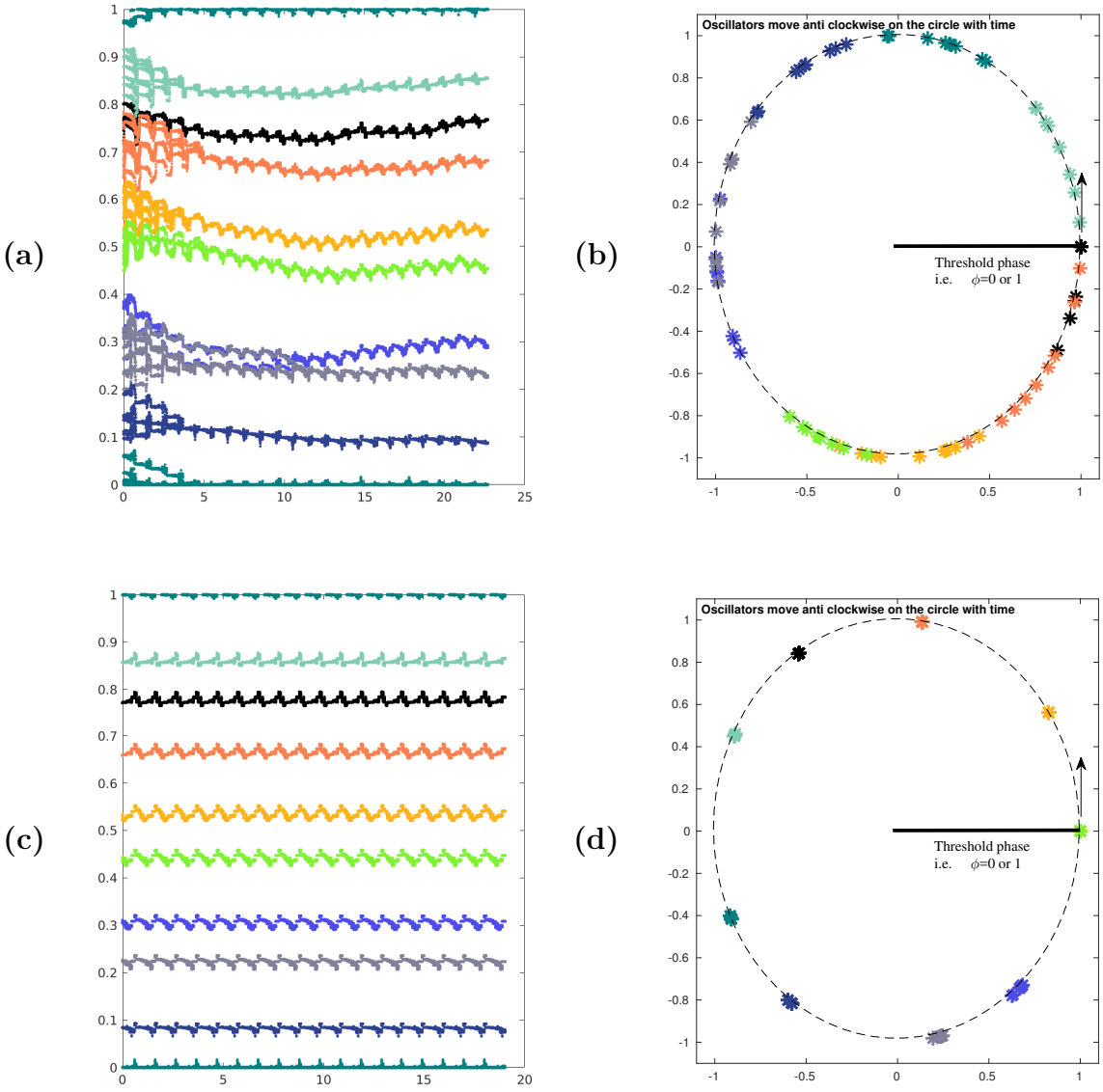

Figure 3.8: Stability of Coloring C (obtained in figures in sections 3.5, 3.6) to phase perturbations. Starting from the state that is associated with a coloring (fig 3.6 (c)), we perturb the phases of the 81 oscillators by $\Delta\bar{\phi} \approx 0.04$ drawn from a Gaussian distribution with mean 0 and standard deviation=.04. MATLAB random number generator(seed=1) was used. We can see that the system returns to the original coloring after some time.

3.5 Stability of Colorings

The states representing colorings obtained after long term simulation of the system are stable to certain order of magnitude of phase perturbations. To demonstrate this, we shift the

phases of the 81 oscillators in a coloring we obtained earlier (Figure 3.5(c) and 3.6(c)) by $\Delta\bar{\phi}$ drawn from a Gaussian distribution with mean 0 and standard deviation=.04. MATLAB random number generator seed=1 was used. The perturbation makes the partitions diffuse (see Figure 3.8 (a), (b)). The system returns to the original coloring after evolution over some events (Figure 3.8 (c), (d)).

In general, colorings obtained are stable up to $\Delta\bar{\phi} \approx 0.05$. A heuristic argument about the stability can be made based on the number of partitions/colors in the system. We have 9 partitions in the system which are going from $\phi_{resting} = 0$ to $\phi^{threshold} = 1$ periodically. So, the average distance between any two partitions of the 9 total partitions is ≈ 0.11. If the perturbation to each neuron ($\Delta\phi$) ≈ 0.05 *or greater*, neurons from different partitions will come close (see Figure 3.9 (b) and they may exchange neurons at the threshold events to arrive at a different coloring (Figure 3.9 (d)).

3.6 Noise Induced Transitions Among Sudoku Solutions

We have shown that starting from random initial conditions, the dynamical system arrives at states characterized by the colorings of the Sudoku graph. Now, we perturb the system at the $2 * 10^4 th$ event i.e. after it has reached the coloring, (see for Figure 3.5 and 3.6 for the coloring before the perturbation). We have used MATLAB rand function with random number generator seed 1 to generate the initial state with an instantaneous phase perturbations $\Delta\bar{\phi}$ drawn from a normal distribution with mean 0 and standard deviation 0.05 (used MATLAB normrand function with random number generator seed 48 for the perturbation).

We can see that the partition colored teal(label 1) and the partition colored violet(label 9) exchange neurons and a different coloring is obtained (Figure 3.9(c),(d) and Figure 3.10). The Sudoku solutions associated with the 2 colorings are shown in Figure 3.10.

For any Sudoku solution (colorings), there are other solutions which may be obtained by exchange of neurons among partitions. The distance between these solutions is measured by the number of minimum exchanges required to go from one solution to the other. Thus,

there is a locality to the dynamical space of our network. We elaborate on this locality in section 4.1.

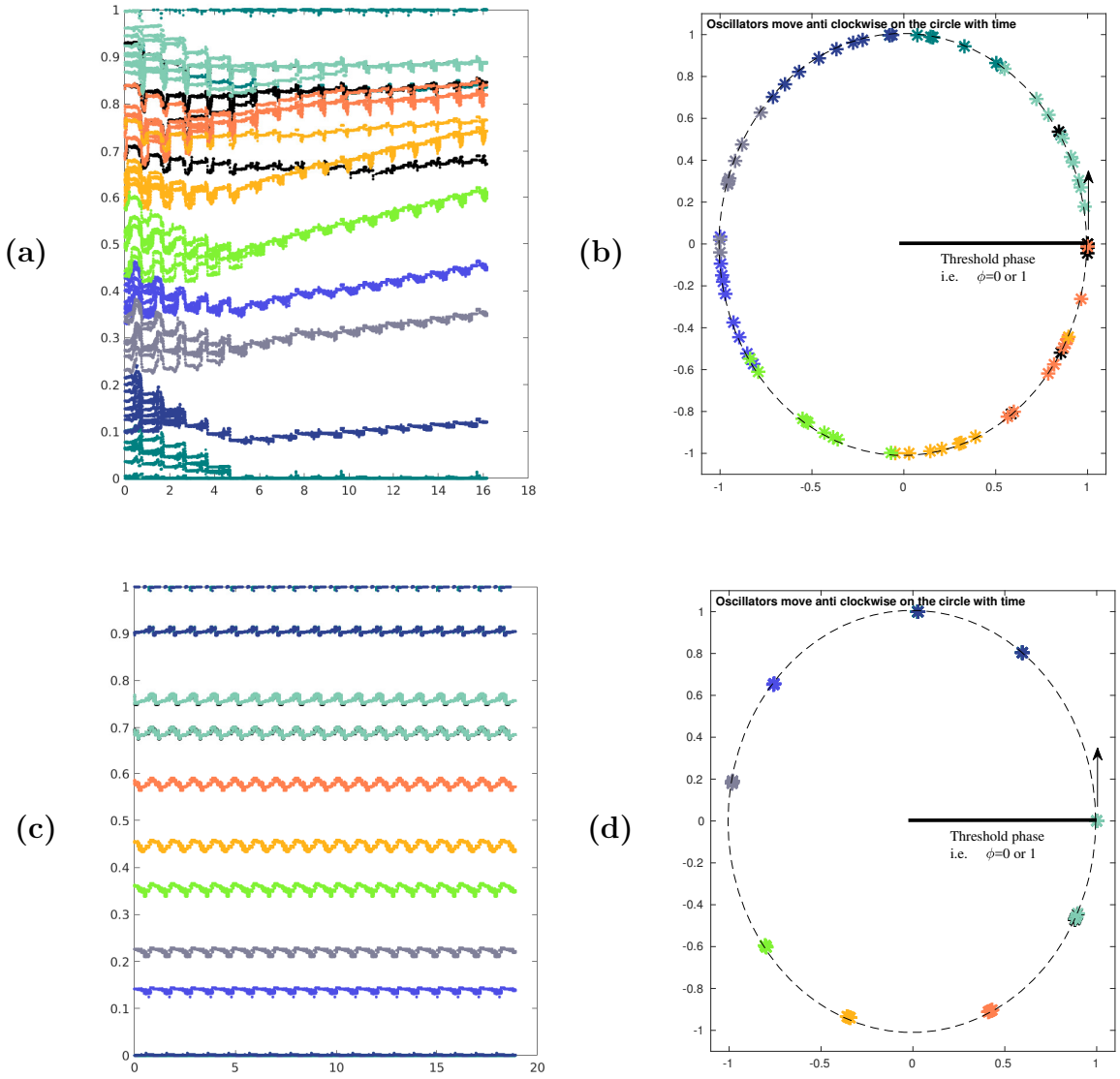

Figure 3.9: Switching to another coloring: Starting from the state that is associated with a coloring (fig 3.6 (c)), we perturb the phases of the 81 oscillators by an instant phase shift give by $\Delta\bar{\phi} \approx 0.05$ drawn from a Gaussian distribution with mean 0 and standard deviation=.05. MATLAB random number generator(seed=1), normrnd function was used. Note that the perturbation is applied exactly at the 20000th event after starting from the the random initial phases random number generator(seed=1).

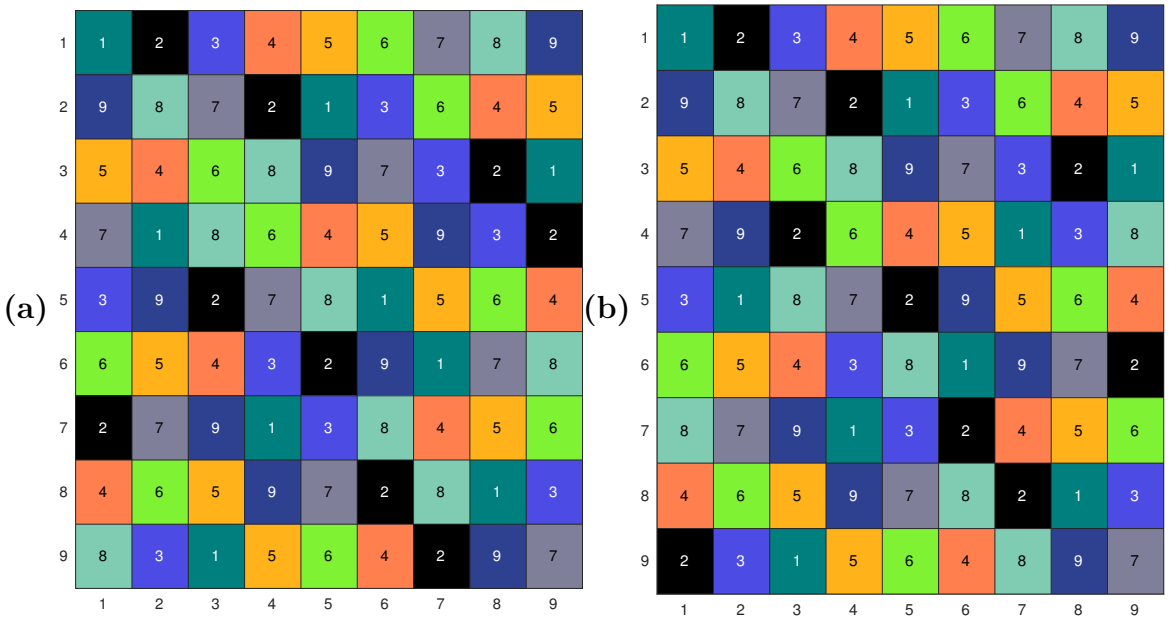

Figure 3.10: Sudoku solutions associated with the colorings: **(a)** Coloring before perturbation, **(b)** Coloring after perturbation. Most of the boxes maintain their color or partition but we can see that the some grids from partitions labelled 1(teal) and 9(violet) have exchanged their positions in the grid. Partitions 2(black) and 8(sky blue) also exchange some elements. The number of exchanges involved in a switching gives us a measure of the distance between the solutions or colorings.

3.7 Description of the dynamical system as a function of Excitation-Inhibition (E-I) ratio

The phase jump ($\Delta\phi$) in the postsynaptic neuron caused by reception of a spike is proportional to the coupling strength ϵ (see figure 2.2).

For sufficiently high values of excitatory coupling ϵ^{exci}, a spike from neuron i, pulls all the neurons $j\epsilon\ Post(i)^+$ to the threshold and therefore, synchronizes these neurons. Here, $Post(i)^+$ is the set of neurons postsynaptic to neuron i with excitatory connection. The set $Post(i)^+$ may include neurons that inhibit each other. Note that if two neurons that inhibit each other spike together, they do not desynchronize upon firing together. So, the inhibitory structural constraints are largely ignored in the dynamics. Thus, for high values of excitatory coupling ϵ^{exci}, we see extreme clustering of neurons, the number of neurons per partition increases and the number of partitions decreases with an increase in ϵ^{exci}.

For low values of excitatory coupling ϵ^{exci}, no reliable clustering of neurons occurs. The 81 neurons stay distributed diffusely from $\phi = 0$ to 1. The pattern we see is that neurons that are immediate neighbors in phase space (neurons next to each other on the circle in figure 3.5 (a)) mostly don't inhibit each other. Let the solutions satisfying the above mentioned constraint be denoted by $S_i^{weak} : i = 1, ..., N_{solutions}^{weak}$ where $N_{solutions}^{weak}$ is the number of dynamical patterns that satisfy this weak constraint. This constraint is much weaker compared to constraints on the dynamics put by graph colorings and $N_{solutions}^{weak}$ much more than the number of patterns allowed by the coloring rule. We point out that stability of these $N_{solutions}^{weak}$ solutions to perturbations goes down for this system as the phase space gets populated by a large number of these solutions and a slight noise can push the system from one solution into the other. We see that the reliability of solutions S_i^{weak} is low for this system with low excitatory coupling ϵ^{exci}.

Thus, we expect a maximization of the number of coloring obtained for a certain ratio of excitation to inhibition. We test this hypothesis in the following section.

3.7.1 Number of Spatiotemporal Patterns as a function of Excitation-Inhibition (E-I) Ratio

We simulate the system for 500 instantiations and observe the asymptotic dynamics and vary the excitatory coupling (c^{exci}) while keeping the inhibitory coupling a constant (c^{inhi}) = $6.5 * 10^{-4}$. Effectively increasing the E-I ratio from left to right (Figure 3.11). We use the algorithm for coloring identification in section 3.4.1 to classify the dynamics of the 500 instantiations as: either a 9-coloring, or Not a 9-coloring.

3.7.1.1 Total number of colorings obtained

We simulate the same 500 initial conditions (chosen randomly, see Appendix for Figure 3.11) for different values of the excitatory coupling (c^{exci}). We keep the inhibitory coupling (c^{inhi}) fixed and thereby study the behavior of our network as a function of the excitation to inhibition ratio ($E - I$ ratio). We observe that the number of colorings (9-colorings) obtained n^{total} maximizes at $c^{exci} \approx$ 4x10^{-}4 (Figure 3.11, (a), Solid line).

If we simulate the same 500 initial conditions for longer time (more events), we see that more of the asymptotic states map to colorings now (Figure 3.11: compare **(a)**1x10^5 events with **(b)** 2x10^5 events and **(c)** 4x10^5 events). So, some states were in a transient and had not settled after the first $1 * 10^5$ events. We expect more of the 500 instantiations will settle to colorings if we allowed the simulations to run longer still.

We perturb the system as shown in figure 3.11 (**(d)**, **(e)** and **(f)**). We note that the number of colorings obtained gets progressively closer and closer to the maximum possible colorings i.e. 500 (which is the total number of instantiations) with more perturbations. The system gets stuck in pathological states which are not colorings. The system can escape these states on the application of a small perturbation (order 0.01) but this perturbation cannot drive the system out of the colorings as the coloring states are stable to perturbations up to order 0.05 (see Section 3.5). Thus, we see this rise in n^{total} upon perturbing the system.

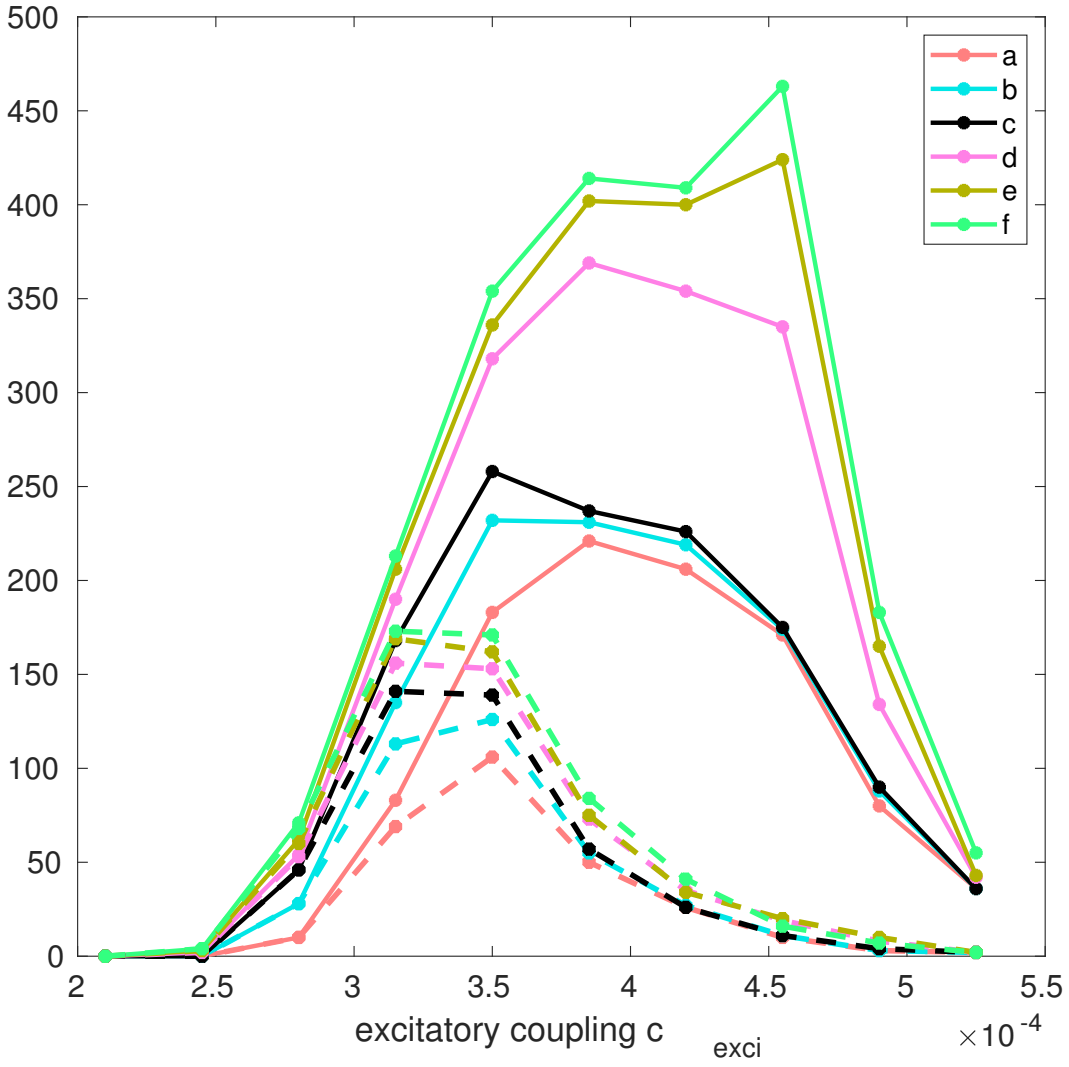

Figure 3.11: X-axis: excitatory coupling c^{exci}. Y-axis (**Solid Lines:**): n_{total}= number of dynamical states that were mapped to colorings using algorithm in section 3.4.2 out of 500 instances, Y-axis (**Dashed Lines:**):- $n^{classes}$= number of classes of colorings (obtained using algorithm in section 3.7.2.1) out of total coloring obtained (solid lines). We evolve the same 500 initial conditions to **(a)**1x10^5 events **(b)** 2x10^5 events **(c)** 4x10^5 events **(d)** 5x10^5 events with a perturbation at the 4x10^5th event **(e)** 6x10^5 events with a perturbation at the 4x10^5th and 5x10^5th **(f)** 6x10^5 events with perturbation every 10^4th event after the 4x10^5th event.

We note that the peaks of the curves in Figure 3.17 (Solid Lines: number of total colorings obtained n^{total}) shift to the right when noise is introduced in the system. System arrives as colorings more often for higher values of excitatory coupling. But note that the peaks for the curves labeled by Dashed lines—representing the number of different classes of colorings $n^{classes}$—do not shift to the right. This is because the increase in the number of colorings for high values of excitation is due to increase in the number of a particular class of colorings $H^{18,27}$ (see section 3.7.2.2).

So, even though the total number of possible colorings n^{total} increases for high excitation c^{exci} (Figure 3.11, solid curves), the variety in the colorings given by $n^{classes}$ decreases (Figure 3.11, dashed curves).

3.7.2 Constructing $J(C)$: Matrix of Inhibitions between Partitions for Coloring C

For any solution or coloring C, a vertex in partition P is connected to 2 or 3 vertices from any other partition $P'(\neq P)$ (See Figure 3.12 for the argument). If N_2 and N_3 are the number of partitions containing 2 and 3 neighbours respectively of a vertex in partition P, then

$2N_2 + 3N_3 = 20$; as the degree of any vertex is 20 and

$N_2 + N_3 = 8$ as the total number of partitions (excluding P) is 8.

Solution to the above equations is $N_2 = N_3 = 4$ i.e. any vertex has 2 neighbours in exactly 4 partitions and 3 neighbours in the remaining 4 partitions.

We define $J(C)$ as the condensed adjacency matrix of a coloring C where $J_{P,P'}(C)$ is the number of inhibitory connections between partition P and P' of coloring C in the Sudoku inhibitory network given by $G(A^{inhi})$ where $P, P' \epsilon \{1, 2, 3, ..., 9\}$.

We see that

- $J_{P,P'}(C) = 18$ when all 9 vertices of partition P have 2 neighbours in partition P', so

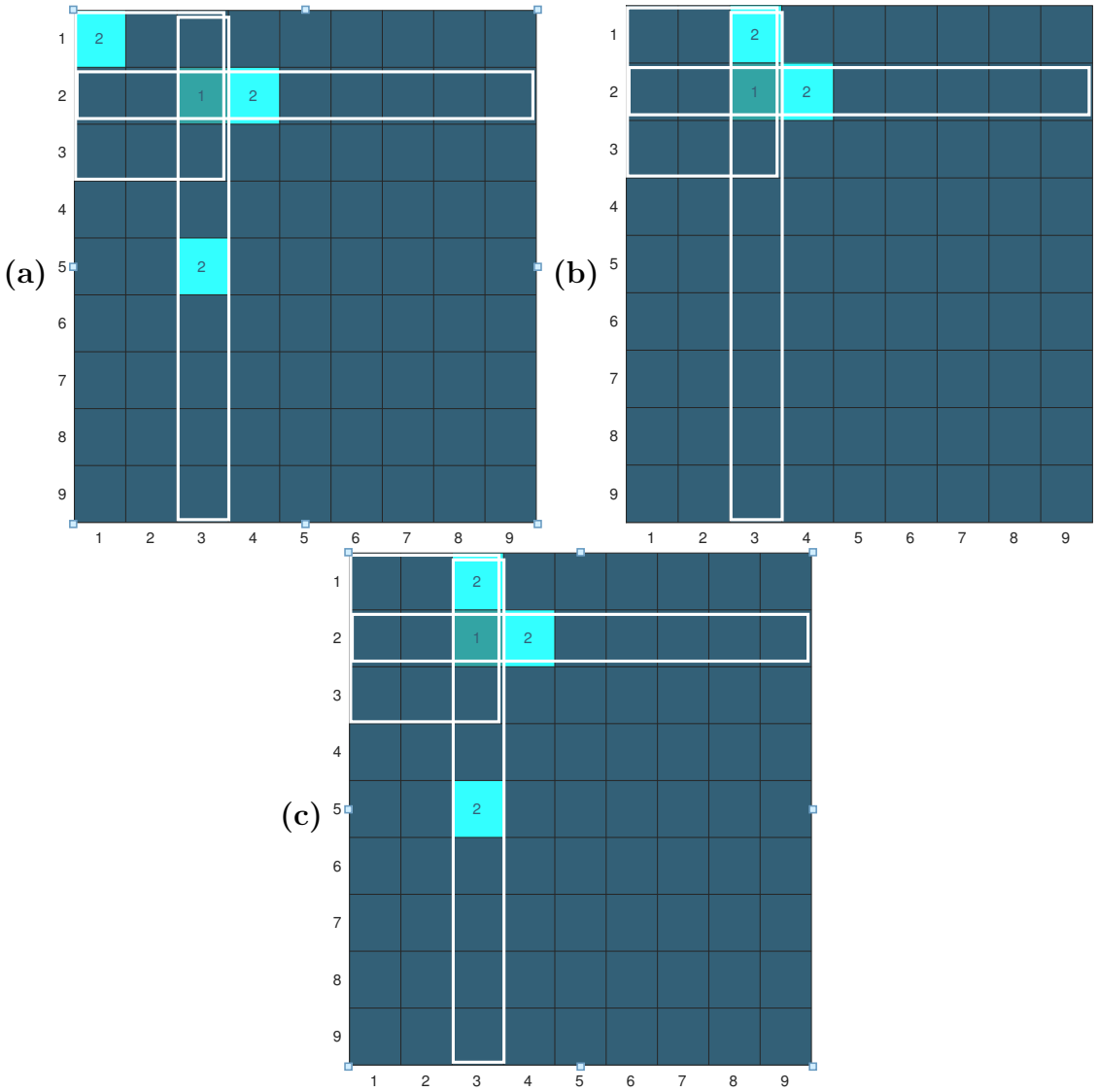

Figure 3.12: Say two partitions in a coloring are represented by labels 1 and 2 as in the figures. Without loss of generality, we place a vertex labeled by 1 at (2,3) and ask how many neighbors can this vertex have in partition labeled by 2. Consider the two vertices in the 3x3 sub-grid at the top left corner of the grid. There are only 2 cases: First, the two vertices labeled by 1 and 2 don't share a row/column **(a)** or they do **(b)**. For cases like **(a)**, the vertex labeled 1 can have 2 more neighbours outside the sub-grid. For cases like **(b)**, the vertex labeled 1 can have only 1 more neighbor outside the sub-grid, otherwise we end up at a situation shown in **(c)**, which is not allowed by the rules of the Sudoku. So, for any Sudoku solution, each vertex in some partition P is connected to either 2 or 3 vertices from any other partition $P'(\neq P)$.

9x2=18;

- $J_{P,P'}(C) = 27$ when all 9 vertices of partition P have 3 neighbours in partition P', so 9x3=27.

It follows that the number of connections between any 2 partitions lies between 18 and 27 (see figure 3.13 (a) for an example of $J(C)$). That is, $18 \leq J_{P,P'}(C) \leq 27 \ \forall \ P, P' \epsilon \{1, 2, 3, ..., 9\}$, $P' \neq P$ for any proper coloring C of G_{Sudoku}. Note, $J_{P,P}(C) = 0 \ \forall \ P \epsilon \{1, 2, 3, ..., 9\}$, as there are no inhibitory connections inside a partition (see Figure 3.7 (a) for an example of J matrix).

3.7.2.1 Types of Colorings based on J matrix

We separate the colorings into classes $\{H_1, H_2, H_3, ..., H_{n^{classes}}\}$ such that colorings belonging to the different classes have different dynamics. We tackle the problem by employing the J matrix of colorings. The method we propose checks whether 2 colorings are different dynamically. This method may fail to resolve some colorings that belong to different dynamical classes and assign them to the same class but it never assigns colorings with the same effective dynamics to different classes. Thus, the number of classes can only be underestimated. To distinguish between different colorings $\{C_i\}$ for $i = \{1, 2, ..., n^{total}\}$ where n^{total} is the total number of colorings, we apply the following algorithm:

- Calculate $J(C_i)$ where C is a coloring of the Sudoku graph G_{Sudoku} for all $i = \{1, 2, ..., n^{total}\}$ using the algorithm in section 3.7.2.
- Evaluate the variance for each of the 9 rows of J excluding the diagonal terms $J_{P,P}$ $(= 0)$. This gives us a variance vector $v(C_i)$ for each coloring C_i; $i = \{1, 2, ..., n^{total}\}$.
- Colorings C_1, C_2 belong to different classes if no permutation of $v(C_1)$ is equal to $v(C_2)$.

Each vertex in the Sudoku inhibitory network has 20 neighbours. For a coloring C_i, the 9 vertices in a partition, say P, the total neighbours are 20x9=180. None of them are inside P (follows from definition of a coloring). It follows that the 180 neighbours are distributed among the other 8 partitions $P'(\neq P)$. Thus, mean of each row (or column) of J is the same $(\sum_{P' \neq P} J_{P,P'}(C_i)/8 = 22.5)$. $J_{P,P'}(C_i)$ with $P'(\neq P)$ represents the number of inhibitory

connections between partitions P and P'. If $\nexists$ a permutation of the partitions of colorings C, C' such that $J(C) = J(C')$, then the dynamics of C and C' cannot be equivalent as the partitions of neurons interact differently for C and C'. Comparing the variance vectors $v(C)$, $v(C')$ is a more computationally efficient way of doing the comparison. The downside is that sometimes $v(C)$ and $v(C')$ can be equal when $\nexists$ a permutation of the partitions of colorings C, C' such that $J(C) = J(C')$ and the colorings are identified as belonging to a single dynamical class. Thus, the algorithm can only underestimate the number of classes $n^{classes}$.

3.7.2.2 Class of Most Occurring Colorings $H^{18,27}$

Largely independent of the noise in the system, we observe that the majority of the colorings that the system settles to are such that $J_{P,P'}$ = either 18 or 27 $\forall$ partitions $P, P' \epsilon 1, 2, ..., 9$. Figure 3.17 shows the fraction of total colorings that satisfy the above mentioned condition on J. We note that the fraction increases as c_{exci} or equivalently c_{exci}/c_{inhi} ($E - I$ ratio) increases.

The reason behind the stability of this class of colorings is structural as well as dynamical. Recall that $J_{P,P'} = 18$ (*or* 27) implies that every neuron of partition P is connected to exactly 2 (or 3) neurons in partition P' (see Figure 3.14). Thus, when the neurons of partition P' spike, all neurons of P get the exact same input –2 (or 3) spikes each for $J_{P,P'} = 18$ (*or* 27)– and the phase difference among the neurons of partition P doesn't increase. This is true for all the partitions if $J_{P,P'} = 18$ (*or* 27) $\forall$ $P, P' \epsilon 1, 2, ..., 9$. Hence, the partitions are tightly clustered and such colorings are highly stable.

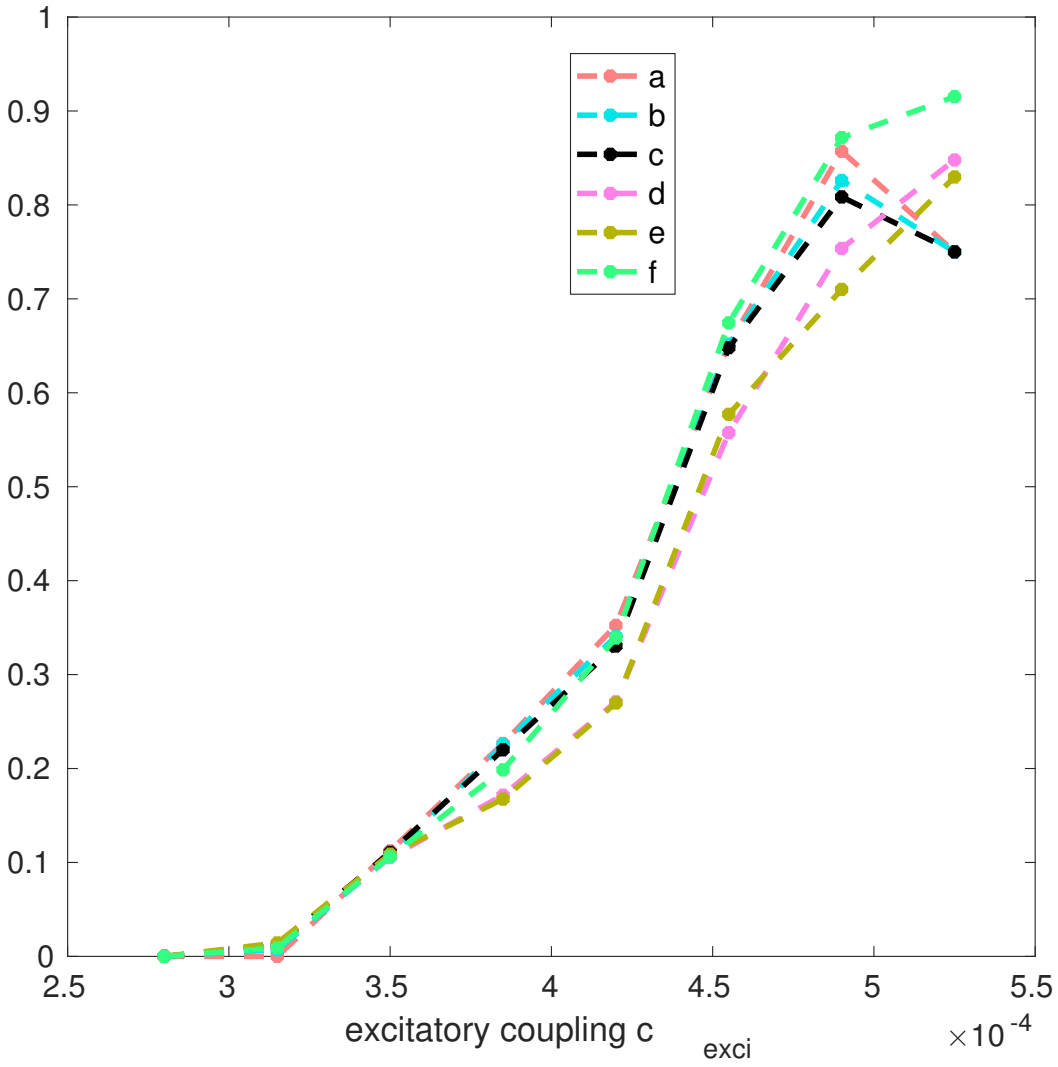

Figure 3.13: Y-axis: Ratio of $n^{18,27}$ to n^{total}; where $n^{18,27}$ is number of colorings with $J_{P,P'} = 18$ or 27 $\forall$ partitions $P, P' \epsilon 1, 2, ..., 9$ (see Section 3.7.2.2) and n^{total} is the total coloring obtained in 500 instantiations of the system. X-axis: c_{exci} We evolve the same 500 initial conditions to **(a)**1x10^5 events **(b)** 2x10^5 events **(c)** 4x10^5 events **(d)** 5x10^5 events with a perturbation at the 4x10^{5}th event **(e)** 6x10^5 events with a perturbation at the 4x10^{5}th and 5x10^{5}th **(f)** 6x10^5 events with perturbation every 10^{4}th event after the 4x10^{5}th event.

Chapter 4

Discussion

4.1 Locality of Response to Perturbations

We have shown that the dynamics of pulse-coupled Sudoku network can be characterized in terms of the colorings of the underlying inhibitory graph. These states are stable to noise(instantaneous) up to $\Delta\bar{\phi}_{perturb} \approx 0.05$. If the perturbation strength $\Delta\bar{\phi}_{perturb} \approx 0.05$ or greater, the system may switch from one coloring say C_i to another coloring C_j. This happens when some partitions of C_i exchange neurons with other partitions of C_i. Then, C_j differs from C_i in that some neurons may change their partitions. For higher values of $\Delta\bar{\phi}_{perturb}$, the system may go to a completely different coloring where the neurons have changed partitions beyond recognition and C_i and C_j seem to have no discernible relation.

Each coloring has a set of neighboring colorings that the system can switch to if a perturbation is given. This way, we can construct a network of colorings and the phase space may be divided into the basins of these colorings. We point out that this *space of colorings* has a sense of locality which may be used to encode distance between inputs. A difference in magnitude of the perturbations (inputs) can be inferred from the number of exchanges that occur among the partitions of a coloring.

Relation to Olfaction and Memory

In the context of the olfactory system, this implies that similar odours might be mapped to similar states (colorings) and odours may be differentiated from each other due to a difference in the perturbation, say input from the Olfactory receptor neurons (ORNs).

In the context of memory, this feature of locality in dynamics relates to the associative property of memory. That is, your next thought (next coloring that the network will arrive at) is decided by your current state of mind (the coloring the network is at right now).

4.2 Benefit of Perturbations

In section 3.7.1, we showed that phase perturbation can drive the system to a coloring more frequently. This might be because the colorings of the system are stable to phase perturbations of order up to 0.05 (see section 3.5 for a heuristic justification) but the states the system gets stuck in—the non-colorings—are not stable to phase perturbations of that order. Thus, the instantaneous perturbations help the systems escape these pathological states and arrive at the colorings.
We have shown that starting from random initial conditions the system arrives at colorings. Thus, the initial randomly chosen state might be in the basin of attraction of the coloring it ends up in. While the coloring is not always a periodic cycle, we still establish that small perturbations O(0.05) do not drive the system away from the states that represent the coloring. Thus, we may argue that colorings are the attractors of this system and the basin size of these colorings O(0.05) is on average bigger than the basins of the non-coloring asymptotic states O(0.01-0.05).

4.3 Functional Role of Excitatory- Inhibitory balance in Neuronal Circuits

Inhibition and excitation seem to hover around a balance in various regions of the brain including but not limited to regions of cortex (Isaacson and Scanziani, 2011) and hippocampus

(Atallah and Scanziani, 2009). There are multiple definitions of this balance but the underlying idea is that the excitatory inputs to a neuron are closely balanced by the inhibitory inputs it receives (Isaacson and Scanziani, 2011; Van Vreeswijk and Sompolinsky).

It's very curious that the brain presses 'the accelerator and the brake' at the same time. Two out of all the hypotheses that have been proposed so far are:

1. Too much excitation can cause unceasing avalanches of spikes (supercritical phase) in the system whereas if the inhibition is too high, the activity dies down too quickly (subcritical phase). The E-I ratio, thus, can be thought as a parameter that can maintain the system at criticality where the state of the system is highly susceptible to input and information transfer in maximized (Beggs and Plenz, 2003; Priesemann et al., 2014; R. Chialvo, 2004).

2. Rubin et al. (2017) claim that it's the encoding capacity of binary neuronal networks that is maximized at a balance of excitation and inhibition as the system is robust to noise in the inputs to the neurons as well as any internal noise in the neurons.

In our system, the number of attractors classifiable as the minimal colorings of the inhibitory network peaks around $c_{exci} \approx 0.00035$ for $c_{inhi} = 0.00065$. The result is true for a range of c_{inhi}. So, if we assume that stimuli are encoded as spatiotemporal patterns representing the minimal colorings, our system also predicts a maximization of encoding capacity at a certain ratio of excitation and inhibition albeit in networks of a pulse coupled continuous neurons.

4.4 Sudoku: A Content Addressable Memory System

Accounting for clues

Clues can be thought of as constraints that disallow some of the $O(10^9)$ solutions/colorings of the empty Sudoku (Herzberg and Murty). In figure 4.1 (d), the number of possible solutions exclude all the solutions where the box labelled by (1,2) and (5,3) contain the same digit s_i,

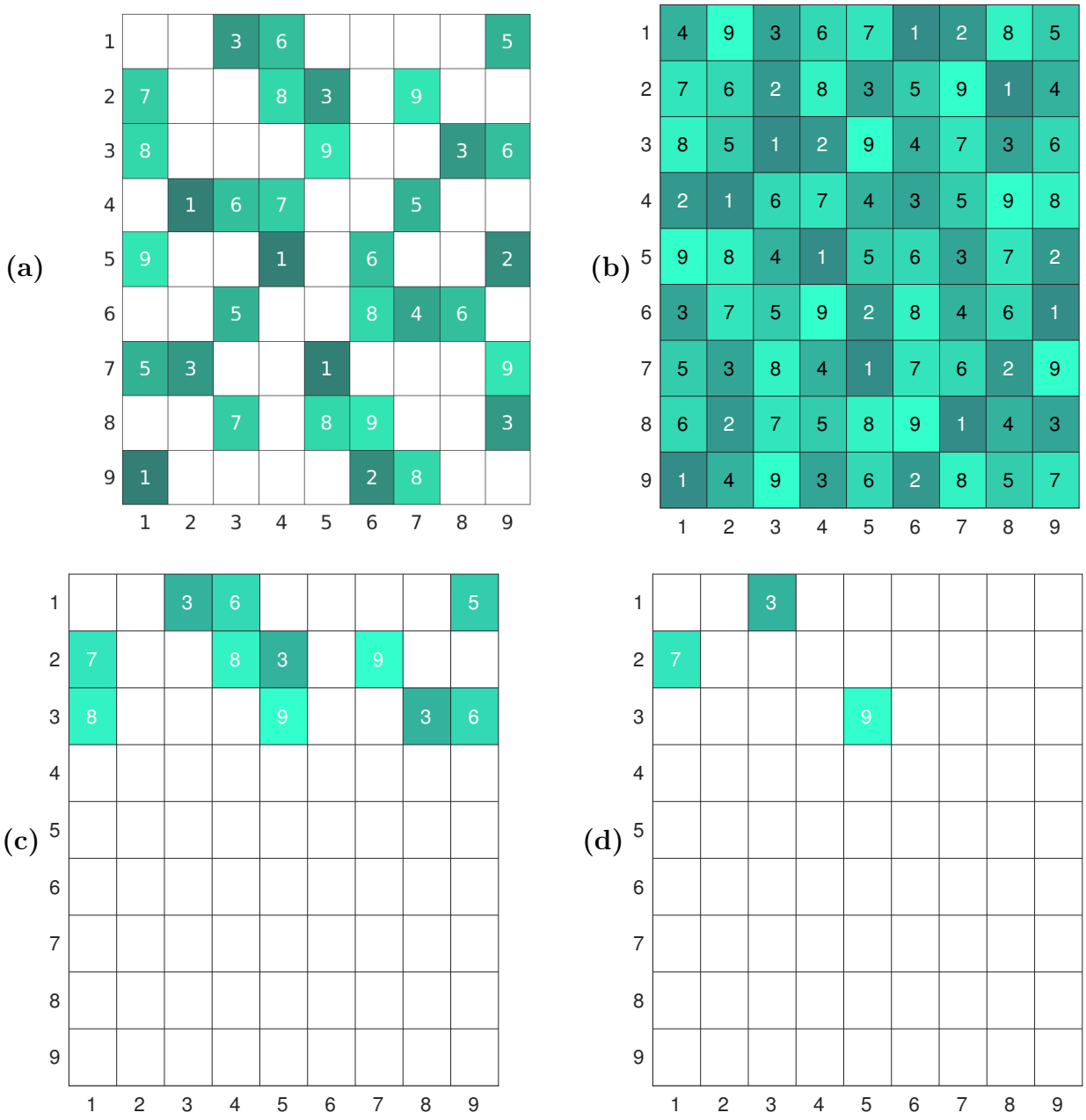

Figure 4.1: **(a)** A Sudoku puzzle with a unique solution, **(b)** the solution of the puzzle in **(a)**. Nothing but the rules of Sudoku are required to arrive at the solution. **(c)** Having fewer clues may may allow more than one solution. **(d)** The box labelled 7 and the box labelled 9 reduce the number of possible colorings from $O(10^9)$.

$i = \{1, 2, ..., 9\}$. Provided enough clues, we end up with a unique solution. Thus, Sudoku can be thought of as a content addressable memory system which outputs the complete pattern(solution) if given enough information about the pattern(clues).

We have thought of some ways to enforce the clues into the dynamical system. First, we explain how clues should affect the dynamics then we show how to force the system to obey the constraints. For the puzzle in 4.1 (d), we see that vertices for boxes (1,2) and (5,3) should **not** share a partition and thus, the associated neurons should "repel" each other in phase space. Instead, if two boxes are labeled by the same number, we need the vertices to be inside the same partition and thus, the associated neurons should "attract" each other in phase space. The clues may be encoded into the adjacency matrices of the inhibitory and excitatory network. When we say encode, we mean that the colorings disallowed by the clues will not be allowed by the adjacency matrix itself. For the puzzle in 4.1 (d), we connect the vertices for boxes (1,2) and (5,3) with an inhibitory edge so that they "repel" and do not share a partition. Instead, if two boxes are labelled by the same number, we connect the vertices with higher excitatory coupling than normal, so that they attract in phase space and be inside the same partition in the dynamics.

The issue is that this addition of edges and selective variation of coupling creates asymmetries among neurons. This doesn't allow the system to have period one dynamics(in which all neurons fire exactly once during a cycle) as neurons in the same partition have different strengths of connections and thus, get desynchronized from the partition.

Bibliography

C. Assisi, M. Stopfer, and M. Bazhenov. Using the structure of inhibitory networks to unravel mechanisms of spatiotemporal patterning. *Neuron*, 69(2):373–386, Jan. 2011.

B. V. Atallah and M. Scanziani. Instantaneous modulation of gamma oscillation frequency by balancing excitation with inhibition. *Neuron*, 62(4):566–577, May 2009.

J. M. Beggs and D. Plenz. Behavioral/Systems/Cognitive neuronal avalanches in neocortical circuits. Technical report, 2003.

A. M. Herzberg and M. R. Murty. Sudoku squares and chromatic polynomials. Technical report.

J. S. Isaacson and M. Scanziani. How inhibition shapes cortical activity. *Neuron*, 72(2): 231–243, Oct. 2011.

G. Laurent. Olfactory network dynamics and the coding of multidimensional signals. *Nat. Rev. Neurosci.*, 3(11):884–895, Nov. 2002.

E. O. Mann and O. Paulsen. Role of GABAergic inhibition in hippocampal network oscillations. *Trends Neurosci.*, 30(7):343–349, July 2007.

E. Marder and D. Bucher. Central pattern generators and the control of rhythmic movements. Technical report, 2001.

R. E. Mirollo and S. H. Strogatz. Synchronization of Pulse-Coupled biological oscillators. Technical report, 1990.

A. Parihar, N. Shukla, M. Jerry, S. Datta, and A. Raychowdhury. Vertex coloring of graphs via phase dynamics of coupled oscillatory networks. *Sci. Rep.*, 7(1):911, Apr. 2017.

V. Priesemann, M. Wibral, M. Valderrama, R. Pröpper, M. Le Van Quyen, T. Geisel, J. Triesch, D. Nikolić, and M. H. J. Munk. Spike avalanches in vivo suggest a driven, slightly subcritical brain state. *Front. Syst. Neurosci.*, 8:108, June 2014.

D. R. Chialvo. Critical brain networks. *Physica A: Statistical Mechanics and its Applications*, 340(4):756–765, Sept. 2004.

R. Rubin, L. F. Abbott, and H. Sompolinsky. Balanced excitation and inhibition are required for high-capacity, noise-robust neuronal selectivity. *Proc. Natl. Acad. Sci. U. S. A.*, 114 (44):E9366–E9375, Oct. 2017.

S. H. Strogatz and R. E. Mirollo. Splay states in globally coupled josephson arrays: Analytical prediction of floquet multipliers. *Phys. Rev. E Stat. Phys. Plasmas Fluids Relat. Interdiscip. Topics*, 47(1):220–227, Jan. 1993.

M. Timme. *Collective Dynamics in Networks of Pulse-Coupled Oscillators*. PhD thesis, Georg-August-Universität Göttingen, Dec. 2002.

C. Van Vreeswijk and H. Sompolinsky. Chaos in neuronal networks with balanced excitatory and inhibitory activity. Technical report.

K. Wiesenfeld and P. Hadley '. PHYSICAL REVIEW LETTERS attractor crowding in oscillator arrays. Technical report, 1989.

Chapter 5

Appendices

5.1 Parameters for Figures 3.5, 3.6, 3.8 and 3.9

Current $I = 1.01$, excitatory coupling $c_{exci} = .00035$, inhibitory coupling $c_{inhi} = .0006$, delay $\tau = .00001$, $\gamma = 1$, frequency $\omega = 1$
T_{free} is the time taken by a non interacting oscillator to fire ($\phi = 1$) staring from the resting phase ($\phi = 0$).

5.2 Parameters for Figures 3.11, 3.13

Current $I = 1.01$, inhibitory coupling $c_{inhi} = .0006$, delay $\tau = .00001$, $\gamma = 1$, frequency $\omega = 1$.

We vary the excitatory coupling c_{exci} for a fixed inhibitory coupling.

The 500 initial conditions (each initial condition is a 81x1 vector of phases of the 81 neurons) were generated using the first 500 seeds of MATLAB random seed generator in the rand function. The perturbations applied in plot 3.11 d,e,f and 3.13 d,e,f were generated using MATLAB normrand function with mean 0 and standard deviation of 0.01. Seed used

was same as the seed used to generate the initial conditions of the neurons. Effectively, the neurons were given instant phase perturbations of magnitude ≈ 0.01.